OULU 2014
C 514

ACTA UNIVERSITATIS OULUENSIS

Maciej Sobocinski

EMBEDDING OF BULK PIEZOELECTRIC STRUCTURES IN LOW TEMPERATURE CO-FIRED CERAMIC

UNIVERSITY OF OULU GRADUATE SCHOOL;
UNIVERSITY OF OULU,
FACULTY OF INFORMATION TECHNOLOGY AND ELECTRICAL ENGINEERING,
DEPARTMENT OF ELECTRICAL ENGINEERING;
INFOTECH OULU

ACTA UNIVERSITATIS OULUENSIS
C Technica 514

MACIEJ SOBOCINSKI

EMBEDDING OF BULK PIEZOELECTRIC STRUCTURES IN LOW TEMPERATURE CO-FIRED CERAMIC

Academic dissertation to be presented with the assent of the Doctoral Training Committee of Technology and Natural Sciences of the University of Oulu for public defence in the OP auditorium (L10), Linnanmaa, on 19 December 2014, at 12 noon

UNIVERSITY OF OULU, OULU 2014

Acta Univ. Oul. C 514, 2014

Supervised by
Professor Heli Jantunen

Reviewed by
Professor Fred Barlow
Professor Marko Hrovat

Opponent
Professor Leena Ukkonen

ISBN 978-952-62-0703-2 (Paperback)
ISBN 978-952-62-0704-9 (PDF)

ISSN 0355-3213 (Printed)
ISSN 1796-2226 (Online)

Cover Design
Raimo Ahonen

JUVENES PRINT
TAMPERE 2014

Sobocinski, Maciej, Embedding of bulk piezoelectric structures in Low Temperature Co-fired Ceramic.
University of Oulu Graduate School; University of Oulu, Faculty of Information Technology and Electrical Engineering, Department of Electrical Engineering; Infotech Oulu
Acta Univ. Oul. C 514, 2014
University of Oulu, P.O. Box 8000, FI-90014 University of Oulu, Finland

Abstract

It has been over a century since the Curie brothers discovered the piezoelectric effect. Since then our knowledge about this phenomena has been constantly growing, accompanied by a vast increase in its applications. Modern piezoelectric devices, especially those meant for use in personal equipment, can often have complicated shapes and electric circuits; therefore, a suitable and cost effective packaging method is needed.

The recent introduction of self-constrained Low Temperature Co-fired Ceramic (LTCC) characterized by virtually no planar shrinkage has pushed the limits of this technology a step further. The practical lack of dimension change between “green” state and sintered ceramic has not only improved the design of multilayer smart packages but also allowed the embedding of other bulk materials within the LTCC and their co-firing in one sintering process.

This thesis introduces a novel method of seamlessly embedding piezoelectric bulk structures in LTCC by co-firing or bonding with adhesive. Special attention is paid to the multistage lamination and post-firing poling of the piezoelectric ceramics. Examples of several structures from the main areas of piezoelectric applications are presented as proof of successful implementation of the new technique in the existing production environment. The performance of the structures is investigated and compared to structures manufactured using other methods.

Integration of bulk piezoelectric structures through co-firing is a new technique with a wide area of applications, suitable for mass production using existing process flow.

Keywords: co-firing, embedded, LTCC, piezoelectric

Sobocinski, Maciej, Pietsosähköisten bulkrakenteiden upottaminen matalan lämpötilan yhteissintrattavaan keraamiin.
Oulun yliopiston tutkijakoulu; Oulun yliopisto, Tieto- ja sähkötekniikan tiedekunta, Sähkötekniikan osasto; Infotech Oulu
Acta Univ. Oul. C 514, 2014
Oulun yliopisto, PL 8000, 90014 Oulun yliopisto

Tiivistelmä

Curien veljekset havaitsivat pietsosähköisen ilmiön jo yli sata vuotta sitten. Ilmiöön liittyvä tutkimustieto ja erityisesti siihen perustuvien sovellusten määrä on nykyisin valtava. Uusissa pietsosähköisissä komponenteissa ja varsinkin niissä, jotka on tarkoitettu henkilökohtaisissa laitteissa käytettäviksi, muodot samoinkuin elektroniikapiirit voivat olla monimutkaisia. Siksi tarvitaan tarkoituksenmukaista ja hinnaltaan edullista laitteen pakkausmenetelmää.

Hiljattain kehitetyt itseohjautuvat matalan lämpötilan yhteissintattavat keraamit (LTCC), joiden planaarinen kutistuma on lähes olematon, ovat lisänneet LTCC-teknologian sovellusmahdollisuuksia. Muotoon valmistetun sintraamattoman ja lopullisen sintratun keraamin dimensioiden yhtäsuuruus ei ole ainoastaan parantanut älykkäiden monikerrospakkausten suunnittelua, vaan mahdollistanut myös erilaisten materiaalien ja komponenttien upottamisen LTCC-rakenteisiin ja niiden yhteissintrauksen.

Väitöstyössä esitetään uusi menetelmä pietsosähköisten bulkrakenteiden upottamiseksi saumattomasti LTCC-rakenteisiin yhteissintrauksella tai liimaliitoksella. Erityistä huomiota on kiinnitetty monivaiheiseen laminointiin ja sintrauksen jälkeiseen pietsosähköisten keraamien polarisointiin. Työssä on esitetty esimerkkejä useista rakenteista pietsosähköisten sovellusten pääalueilta osoituksena uuden tekniikan onnistuneesta käyttöönottamisesta nykyisessä valmistusympäristössä. Tutkittujen uusien rakenteiden ja muilla menetelmillä valmistettujen rakenteiden ominaisuuksia on verrattu keskenään.

Pietsosähköisten bulkrakenteiden integroiminen yhteissintrauksella on uusi tekniikka, joka mahdollistaa lukuisia sovelluksia ja soveltuu massatuotantoon olemassa olevilla prosseintilaitteistoilla.

Asiasanat: LTCC, pietsosähköinen, upotettu rakenne, yhteissintraus

To my friends and family.

Acknowledgments

There would be very little written in this book if not for my parents and grandmother, who raised me, steering my life through the changing winds of youth, or if teachers at all educational levels had not shown me the marvels of science.

This thesis certainly would not exist if it were not for the Erasmus Exchange program and Professor Leszek Golonka, who made the bilateral agreement with the University of Oulu or professor Heli Jantunen, who gave me the opportunity to be part of the Microelectronics and Material Science Laboratories, and Jari Juuti, who has carefully guided me through the world of science during the seven years since I came to Finland.

Much of the research presented here would not have been possible without the support of my colleagues who were tireless in answering all my questions. Much of the quality of the thesis would be lost if not for the people working in Microelectronics and Material Science Laboratories, as the great atmosphere they create makes it easy to come to work every day.

None of this would have been possible without my friends, who kept me sane and happy, even when it rained and there was minced liver for lunch. I must also mention the special care given to me by the one and only Marta, my fiancé, best friend, and first mate on the ship of my life.

I also wish to thank the Tekniikan Edistämissäätiön, Nokia Scholarship Foundation, Oulu University Scholarship Foundation and Infotech who supported me financially.

Without all of you, and many others it would not have been possible…

List of abbreviations and symbols

AFM	Atomic Force Microscopy
BST	Barium Strontium Titanate
CTE	Coefficient Of Thermal Expansion
LTCC	Low Temperature Co-fired Ceramic
MEMS	Micro Electro Mechanical Systems
KNB	Sodium Potassium Niobate
PCB	Printed Circuit Board
PVDF	Polyvinylidene Fluoride
PZT	Lead Titanate Zirconate
QMB	Quartz Micro Balance
RF	Radio Frequency
SAW	Surface Acoustic Wave
SVM	Sacrificial Volume Material
USG	Ultrasonography
PS	Spontaneous Polarization
PR	Remanent Polarization
d	Piezoelectric Coefficient
Q	Quality Factor
μTAS	Micro Total Analysis System

List of original papers

Original papers are referred to throughout the text by their roman numerals.

I Sobociński Maciej, Zwierz Radoslaw, Juuti Jari, Jantunen Heli, Golonka Leszek (2010) Electrical and electromechanical characteristics of LTCC embedded piezoelectric bulk actuators. Advances in Applied Ceramics, 109.

II Sobocinski Maciej, Leinonen Mikko, Juuti Jari and Jantunen Heli (2011) Monomorph piezoelectric wideband energy harvester integrated into LTCC. Journal of the European Ceramic Society, 31(5)

III Sobocinski Maciej, Leinonen Mikko, Juuti Jari, Jantunen Heli (2012) A Piezoelectric active mirror suspension embedded into Low Temperature Co-fired Ceramic. IEEE Transactions on Ultrasonics, Ferroelectrics, and Frequency Control, 59 (9)

IV Sobocinski Maciej, Leinonen Mikko, Juuti Jari, Mantyniemi Noora, Jantunen Heli (2014) A Co-fired LTCC-PZT monomorph bridge type acceleration sensor. Sensors and Actuators A, Physical, 216

V Sobociński Maciej, Juuti Jari, Jantunen Heli, Golonka Leszek (2009) Piezoelectric unimorph valve assembled on an LTCC substrate. Sensors and Actuators. A, Physical., 149 (2)

Paper I presents the co-firing method of integrating bulk piezoelectric parts made of Lead Zirconate Titanate (PZT) in LTCC, and evaluates the electromechanical properties of such structures. Using a laser, commercially available PZT discs are cut in round and rectangular shapes, placed between layers of commercially available, non-shrink LTCC and co-fired. The influence of co-firing on electromechanical properties is investigated and necessary modifications to LTCC process flow are discussed.

Papers II – IV present PZT-LTCC structures in the application areas of energy harvesters, actuators, and sensors respectively. In Paper II a PZT structure for energy harvesting with three beams of different length is cut out from a commercially available disk, laminated with LTCC packaging and co-fired. The different lengths of the beams provide the structure with wideband resonance frequency characteristics. Each of the resonance frequencies is measured and the bandwidth is calculated. Power generation per one g of acceleration is calculated and the optimum load resistor was selected. The influence of packaging is investigated and compared to the unpackaged reference sample.

In Paper III a PZT-LTCC active suspension for a portable Fabre-Perrot Interferometer is presented. The co-fired structure has three PZT arms joined together in the middle by an LTCC mirror holder, whereas the second mirror, needed to form the optical resonance chamber, is placed on the top of the package. The three moving arms allow changing of the distance between the mirrors, which allows the structure to change its output wavelength. Furthermore, moving arms make the fine-tuning of mirror parallelism possible. The Paper presents the tuning capabilities of the structure, together with resonance frequency measurements and stabilization times.

Paper IV presents an accelerometer consisting of a two arm piezoelectric sensing structure and LTCC package. A PZT element shaped out from a single disk is embedded in LTCC package. The sensing arms are connected by the LTCC mass suspended on thin, hinge-like structures. This solution provides robustness and resistance to in-plane accelerations, maintaining higher sensitivity in the designated direction then a single PZT beam supported from two sides. Measurements include investigation of sensitivity, linearity and selectivity as well as response time.

Paper V shows bonding with adhesive as a feasible method for the integration of bulk PZT disk on LTCC substrate for microfluidics application. Mounting the PZT disk in a post-firing process allows the use of LTCC material that is not non-shrinking, and does not require post-firing poling. Moreover, the sintered LTCC is rigid and allows moulding of the steel membrane by pressing it against the ceramic. This allows minimization of the distance between the membrane and the valve seat, which results in lower leakage in the closed state and faster closing times.

The author’s input into these five papers includes the design of the LTCC parts, the manufacture of the structures and their measurements. The author wrote and edited the manuscripts with the kind help of the co-authors, excluding the parts describing simulations that the co-authors wrote themselves.

Table of contents

1 Introduction

Piezoelectric components play a key role in modern electronics. The high demand comes from their ability to transform mechanical energy into electric one and vice versa with high effectiveness as well as the vast span of application the both effects have. Their applications, ranging from hand-held, everyday-use electronics to complex structures working in the harsh environment of outer space, require reliable, functional and cost effective packaging. Growing complexity and novel applications often surpass the capabilities of traditional packaging methods demanding smaller connector pitch, denser interconnections and better functionality; therefore, a new approach is needed. On the other hand LTCC technology expands to novel areas of applications including sensors, actuators and microfluidics. These new applications require embedding of novel functional materials and developing new methods for the integration. According to ScienceDirect the interest in researching piezoelectric structures in LTCC, presented in Fig. 1, is growing periodically. However, very little research is conducted into successful combining these two technologies together.

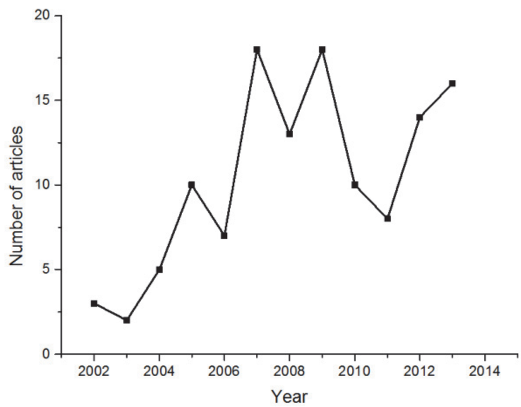

Fig. 1. Number of publications containing the word "piezoelectric" and "LTCC" in the function of time (collected 20.01.2014).

1.1 Piezoelectricity and its applications

The piezoelectric effect was discovered in the 19^{th} century by Jacques and Pierre Curie. They noticed that certain crystals generate electrical charge when subjected to external stress: this has been named the direct piezoelectric effect. Not long after, Gabriel Lippmann gave the theoretical basics for the converse piezoelectric effect (that is, deformation of the crystal under applied voltage), and this effect has been later practically proven by the Curie brothers.

The 20th century has brought the fast development of new piezoelectric materials and applications. The sonar, the phonograph, piezoceramic filters for radios and televisions, audio transducers that can connect directly to electronic circuits, and perhaps the most often used application - the piezoelectric igniter. The ongoing scientific revolution has brought new applications to both industry and the home market, such as precise positioning systems, Surface Acoustic Wave (SAW) filters, ultrasonic motors, Ultrasonography (USG) 3D imaging systems, household inkjet printers, proximity sensors for cars and skis with piezoelectric dampening systems. Nowadays, piezoelectric applications are present in equipment such as sensors (accelerometers, vibration, SAW, microbalance), actuators (laser positioning, camera auto-focus, wafer and mask positioning) and energy harvesters (vibration, impact, clothing). Furthermore, scanning microscopes that allow us to see the nano-world, like the Atomic Force Microscope (AFM), are based on piezoelectric effect (Cady 1964, Jaffe et al. 1971, Uchino 2000).

Research on piezoelectricity started with naturally occurring crystals like topaz, tourmaline and quartz. World War II brought polycrystalline ceramic materials such as barium titanate, but the real revolution happened when Lead Zirconate Titanate (PZT) was introduced. Nowadays, strict policies against the use of lead push scientists towards different materials like sodium potassium niobate (KNB) or piezoelectric polymers such as polyvinylidene fluoride (PVDF).

The future of piezoelectricity seems to be bright, with new materials and new applications being presented every year.

1.2 LTCC and its applications

LTCC is an important packaging technology in today’s microelectronics. It was developed in the 20th century starting as a simple multilayer substrate technology designed to work with highly conductive metals such as silver and copper. Since then, it has undergone many changes, and evolved into sophisticated packaging technology capable of integrating passive components within complex 3D structures (Imanaka 2005).

The LTCC system usually consists of dielectric tapes, and different thick film pastes for screen-printing, which are compatible with the tapes in chemical, electrical and mechanical ways. Dielectric tapes are commonly prepared from fine powders of ceramics and glass mixed together with organic binders, solvents and other additives. These complex mixtures, prepared in the form of homogenous slurry, are then tape-cast onto polymer support tapes through a doctor blade that defines the thickness of the tape (Mistler & Twiname 2000). Dried and cut or rolled sheets are delivered to customers in "green" (i.e. unsintered) state. Thick film pastes are usually conductive, resistive or dielectric, but the development of approaches to manufacture novel pastes are ongoing. Recent innovations in this area include PZT pastes (Hrovat *et al.* 2006) and Barium Strontium Titanate pastes (BST) (Tick *et al.* 2008). Pastes are made from functional powders mixed with binders and solvents compatible with those used in the green tapes. Screen-printing requires the pastes to demonstrate thixotropic behaviour, that is, to change their rheological behaviour during printing. When subjected to shear stress, pastes become more fluid and reclaim their high viscosity once they are on the substrate. This ensures ease of printing but also well-defined prints and minimal bleeding (Imanaka 2005).

In modern LTCC technology, applications have been adopted from packaging, RF components, the automotive industry and space technology. Current research is focused on finding new, functional materials as well as new applications, in fields such as microfluidics, microsystems, sensors and actuators.

1.3 Objective and scope of the thesis

The objective of this thesis is to present the possibilities for the direct embedding of bulk piezoelectric structures in LTCC as a new way of packaging and introducing novel functionality to the LTCC technology. The focus is on manufacturing and evaluating different structures and their performance in the main areas of piezoelectric applications with special attention put on integration through co-firing.

Chapter 2 presents a literature study of piezoelectric components from the application areas presented in this thesis, discussing their design, performance, packaging and means of mounting to substrates.

Chapter 3 focuses on the process of embedding piezoelectric structures in LTCC, covering manufacturing methods, benefits and drawbacks, challenges of both adhesive bonding and co-firing and the performance of manufactured structures.

Finally, Chapter 4 summarizes the results and presents the possible impacts on science and industry.

2 Materials

Piezoelectric bulk components can be manufactured from many materials, however it is PZT that dominates the market. Its ease of manufacture, versatility, and excellent piezoelectric properties, together with its cost-efficiency, made it the perfect focus material for this thesis. A commercial PZT Pz29 manufactured by Ferroperm Piezoceramics A/S has been chosen as the excellent example of high performance piezoelectric material. All five papers present research using this material in the form of different structures trimmed from thin disks with silver thick-film electrodes on both sides.

For the research activities presented in papers I-IV, HeraLock 2000 LTCC (available from Heraeus) has been chosen for its remarkable, near-zero planar shrinkage, which was essential for co-firing. During the research presented in Paper V, DuPont 951 LTCC has been used due to its well-known behaviour and well-established processing methods. This chapter presents detailed information about the materials used.

2.1 PZT ceramics

In piezoelectric ceramics, which fall within the scope of this thesis, macroscopic piezoelectric properties have to be induced externally due to their polycrystalline structure. When cooling down from the paraelectric state, crystals building the ceramic become ferroelectric, usually elongating along the polar axis. The stress caused by changes in the dimensions of grains is minimized by the formation of domains (regions with the same direction of spontaneous polarization). However, the spontaneous polarization might differ between the domains, resulting in overall cancelation of the macroscopic polarization, thus cancelation of the piezoelectric properties of the bulk structure. In order to obtain macroscopic piezoelectric properties, the domains need to be aligned in one direction. This so-called poling is done by applying a high electric field, which switches the domains along the direction of the applied field. Poled ferroelectric ceramic can behave as a single body showing piezoelectric properties along the poling axis (Jaffe *et al.* 1971).

PZT is a solid solution of $PbZrO_3$ and $PbTiO_3$ having a perovskite-type crystalline structure with the highest piezoelectric properties at the morphotrophic phase boundary: i.e. at the chemical composition where both crystalline phases (the rhombohedral phase and the tetragonal phase), co-exist together.

One of the advantages of PZT materials is the user's ability to tailor the material's properties to their needs either by changing composition, by doping, or by adding another perovskite to the solid solution creating a ternary system.

The most common method of manufacturing PZT materials is the oxide mixing method. In this method, the oxide powders are mixed with each other and with organic additives like binder and either pressed into pellets, tape-cast in the form of slurry, or screen-printed as a paste. The PZT discs used in this thesis were manufactured by Ferroperm Piezoceramics A/S as shown on Fig. 2. First, raw materials are mixed in the right proportions forming a uniform mixture. Next, the mixture is thermally processed in order to form a crystalline phase, which is then milled again. Following that, the mixture is mixed with binder, and pressed into disk shape. Finally, the binder is burnt out at 700 ºC, followed by sintering in the temperature between 1200 and 1300 ºC (Ferroperm Piezoceramics, 2013).

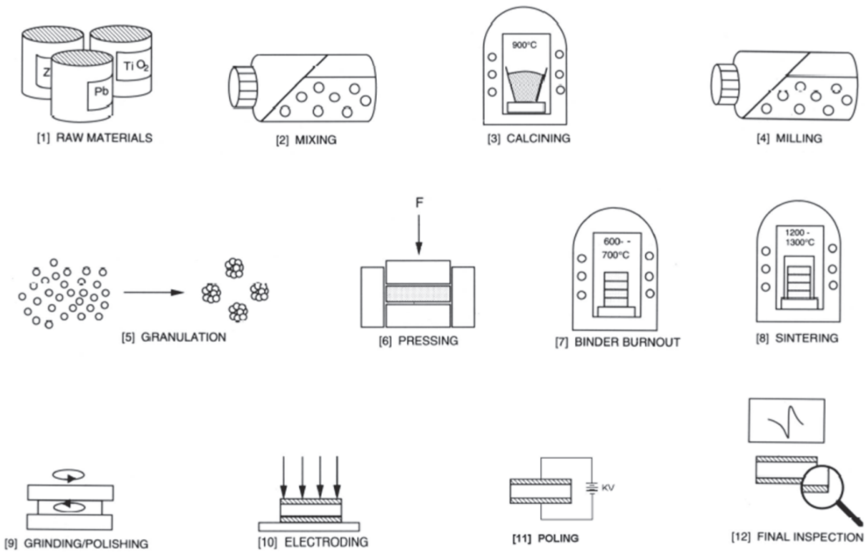

Fig. 2. Process flow for manufacturing PZT disks of Ferroperm resulting in dense, high performance piezoelectric disks ready for further processing. In case of co-firing, steps 10 – 12 can be omitted, as electrodes could be printed on LTCC and poling has to be done after co-firing (Ferroperm Piezoceramics, 2013). Reprinted with permission from Ferroperm Piezoceramics.

After sintering, the parts are grinded, lapped and polished in order to match the required dimension tolerances. Electrodes are applied, through screen-printing or vacuum deposition. Next, the PZT parts are poled in order to establish uniform direction of polarization. Final inspection is carried out 24h after poling and includes measuring of the dielectric and piezoelectric properties and the adhesion of the conductive layer (Ferroperm Piezoceramics, 2013). Such process flow allows the creation of various shapes, depending on the mould used in dry pressing. Rings, tubes, plates, rods, focusing bowls and other shapes are possible. Pz29 chosen for this thesis is a “soft” PZT composition with high coupling coefficients and dielectric constant excellent for vast spectrum of applications. Chosen dielectric and piezoelectric properties are shown in Table 1.

Table 1. Chosen properties of Pz29 PZT (Ferroperm Piezoceramics, 2013).

	Dielectric constant @ 1 kHz	Dielectric dissipation factor @ 1 kHz	Curie Temperature ºC	Coupling factor k_p k_t k_{31} k_{33}	Piezoelectric charge coefficient d_{31} d_{33} d_{15} [pC/N]	Piezoelectric voltage coefficient g_{31} g_{33} [Vm/N]
Pz29	2900	0.019	235	0.64, 0.52, 0.37, 0.75,	-240, 575, 650	-10, 23

2.2 LTCC

During the 1980s, LTCC technology was introduced as a multilayer substrate technology for RF applications (Imanaka 2005). Thirty years later, the use of LTCC has spread across many different application fields. Vendors such as DuPont, Heraeus Holding GmbH, ESL ElectroScience and Ferro Corporation now offer LTCC systems for sale, while some companies such as Kyocera Corporation and Murata Manufacturing Co. Ltd use their own ceramic systems in their manufacturing of advanced ceramic components. Before the introduction of self-constrained LTCC tape, large shrinkage of the ceramic during sintering induced stress in any bulk material that was being co-fired. Although the internal stress in some cases could be used in favour of the piezoelectric structure as reported by Juuti *et al.* (2006) and Heinonen *et al.* (2007), generally co-firing caused destruction of any bulk material inserted between the tapes. Alternative methods of reducing planar shrinkage, such as pressure assisted sintering, could be harmful for complex 3D structures and might need additional process steps when i.e. using DuPont’s constraining release tape. In 2004 Heraeus GmbH has patented a self-constrained tape called HeraLock 2000, which exhibits virtually no planar shrinkage (Lautzenhiser et al. 2004). The minimal 0.2% shrinkage in the x-y plane has been possible thanks to the multilayer structure of the tape (Fig. 3) (Rabe et al. 2005).

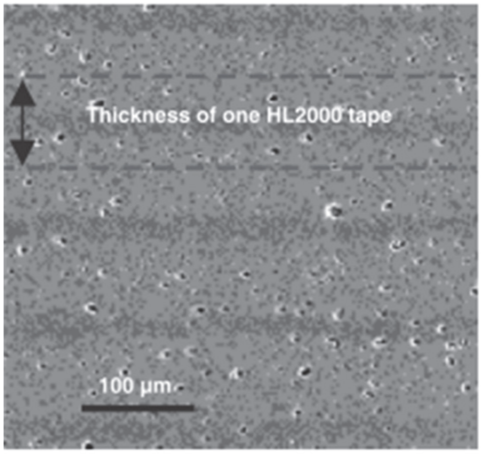

Fig. 3. Cross-section through HeraLock 2000 LTCC with the three-layer building of each of the tapes easily visible: inner refractory ceramic layer and two layers of a mixture of crystalline powder and low-melting-point glass on top and bottom. The three-layer build gives the tape its “non-shrinking” properties (Rabe *et al.* 2005). Reprinted with permission of John Wiley and Sons.

According to Rabe *et al*. (2005), each sheet of HeraLock 2000 consists of inner refractory ceramic layer and two layers of mixture of crystalline powder and low melting point glass on top and bottom of the refractory ceramic, manufactured with wet-on-wet tape casting method. During sintering, low melting glass phase in the outer layers softens and begins to flow into the middle layer drawn by capillary forces. The shrinkage necessary for densification is done completely in the z direction that is currently reported by the datasheet to be at the level of 32% for 131 μm thick tapes. (Heraeus 2013)

HeraLock zero shrinkage ceramic tape has allowed successful experiments on seamless integration of piezoelectric bulk structures with LTCC through co-firing in projects conducted by the author, and by Flossel *et al.* (2009). Furthermore, it has been shown that the HeraLock 2000 process flow needs only small adjustments to facilitate this integration, meaning that the existing production lines can be used to manufacture novel PZT-LTCC structures. A detailed description of the process is presented in Chapter 3.2.

3 Embedding of bulk piezoelectric components in LTCC

Piezoelectric components, like all electronic devices need to be connected electrically and mechanically to the system in which they are working. Commercially available PZT bulk elements are available in various packages depending on their use, or have no packaging at all. Industrial and heavy-duty sensors are usually provided with large, durable steel packages that are screwed directly to chassis and connected electrically with separate cables. However, smaller sensors or actuators are rarely available with packaging suitable for surface mounting on a printed circuit board (PCB). Moreover, there is little ongoing research into the integration of PZT bulk parts with electronics on the packaging level. Actuators such as those manufactured by Noliac A/S can come without any packaging at all – an issue that has to be addressed immediately after purchasing. Other companies such as Physik Instrumente (PI) GmbH & Co offer certain piezoelectric actuators in a package, but the majority of their range is sold bare. Mounting for these devices has to be done via adhesive bonding or soldering and severe damage might be dealt to the structure if mounting is not carried out correctly. The need for a package is justified not only by the need of electrical and mechanical connection of the bare piezoelectric structure, but also by the need of protecting the structure from ambient conditions and accidental damage during handling.

3.1 Adhesive bonding and soldering

Adhesive bonding and soldering was tested by Fournier *et al.* (2007) in an attempt to manufacture a bulk PZT bending actuator, which could then be used in LTCC based valves and pumps for the meso-scale microfluidics systems. This would replace the thick film structures, which were investigated by Santo *et al.* (2005) and proved inefficient due to high stiffness of ceramic substrates. Testing of several glues and solders concluded overall better performance of glue over solder due to lack of the risk of PZT depolarisation linked to high temperature during soldering. On the other hand, bonding with adhesive comes with the problem of long time stability, reliability and vulnerability to external conditions such as moisture.

Precise positioning and distance management is an issue that has been investigated in Paper V where a PZT-Steel unimorph was glued on LTCC substrate forming a valve (Fig. 4). Leakage problems were caused by the unknown and hard to manage distance between the moving membrane and the valve seat. Furthermore, excessive amounts of glue clogged the valve before a special reservoir was designed.

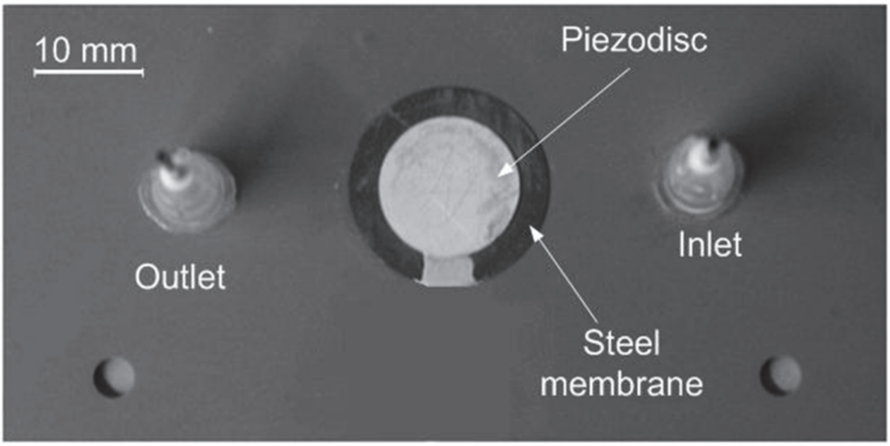

Fig. 4. Photograph of valve assembled by bonding with adhesive. The piezoelectric disc (diameter 12 mm) and the steel membrane (diameter 17 mm) form a bending unimorph which when submitted to electric field closes the via in the valve seat cutting the flow (Paper V). Reprinted with permission of Elsevier.

3.2 Co-firing

Juuti *et al.* (2006) and Heinonen *et al.* (2007) have investigated earlier integration of bulk PZT components with LTCC through co-firing. In these investigations, the focus was on the performance enhancing influence of the DuPont 951 LTCC passive layer in pre-stressed bending actuators. However, the 15% planar shrinkage of DuPont 951 LTCC made it very challenging to manufacture a complete package for the PZT structure. The introduction of zero-shrinkage HeraLock 2000 LTCC tape allowed the first true co-firing integration as shown in Papers I-IV and in works by Flossel *et al.* (2009).

The typical LTCC process illustrated in Fig. 5 starts with blanking the tapes, cutting them to suitable size, and forming vias and cavities. Next, the vias that connect the tapes vertically are filled with conductive paste. This is followed by screen-printing of electrical circuits on top of the tapes. Then the tapes are stacked - using either optical alignment or register pins, tacked together either by drops of alcohol or hot irons - and vacuum bagged. Bags are then laminated according to the specifications delivered by tape manufacturers – usually 10 minutes at 75 °C and 100 – 200 bar pressure. At this stage, the samples lose their tape structure and become uniform bulk material. After removal from the lamination bags, LTCC can be sintered in a variety of furnaces according to the sintering profile provided by the vendor. Typically, this step takes from a few to several hours depending on the tape and the furnace, with the peak temperature commonly reaching 850 °C. Finally, post-processing can be done including additional screen printing, soldering and dicing.

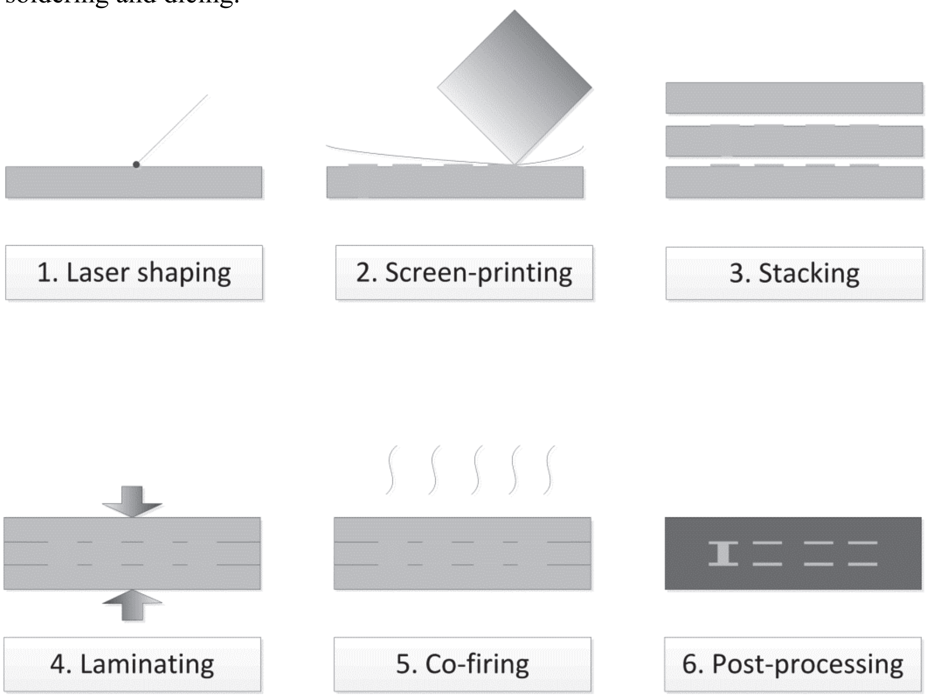

Fig. 5. LTCC process flow common for all LTCC systems. Differences might occur due to tape properties during lamination and co-firing. Laser shaping is used to blank the tape and drill conductive vias, and might be substituted by mechanical cutting/punching. Screen printing fills vias with paste and creates circuitry. Several prints on one tape are possible, each finished with drying. Stacking and laminating forms the 3D structure and makes the layered structure into one body. During co-firing, organics are burnt out, and the ceramic sinters, obtaining its final mechanical and electrical properties. Post-processing might include further screen printing followed by sintering, dicing, surface mounting, etc.

In order to co-fire PZT structures in LTCC changes to the process flow need to be carried out. These include the insertion of the bulk PZT structure during stacking, multiphase lamination, extending the lamination time and poling after sintering.

A piezoelectric structure that is to be embedded in LTCC through co-firing should be first shaped according to the design and cleaned from any contaminations. For better results, the LTCC should be cut in such a way that the stacked tapes form a cavity with dimensions corresponding to the shape of the PZT structure, so when the PZT part is inserted into the cavity during stacking, all the sides are tightly matched. This will ensure the correct alignment and will prevent the structure from moving during handling prior to lamination. An example of stacked LTCC tapes and PZT bulk structures is shown in Fig.6.

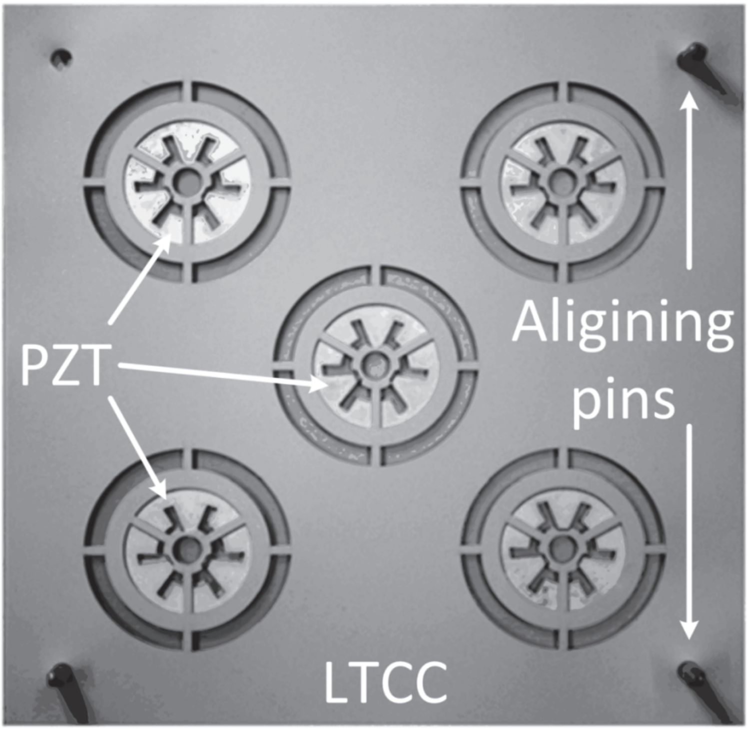

Fig. 6. Stacked LTCC tapes and bulk PZT structures prior to lamination. 4 mm aligning pins are used to stack the 88 mm x 88 mm tapes with an accuracy of up to +/- 12.5 μm. Five cavities 250 μm deep were cut out in order to facilitate PZT components that were 15 mm in diameter. 2 mm wide trenches around the cavities were cut to ease the dicing (Modified from Paper III). Reprinted with the permission of IEEE.

The amount of LTCC tapes needed to form the cavity depends on the thickness of the piezoelectric element. The tapes should be set up in such a way that the top surface of the piezoelectric element is as close to the level of LTCC surface as possible (e.g. for structures 375 µm thick three 130 µm tapes should be used). If the difference of surface levels is too large, lamination will not proceed correctly resulting in blistering, cracking or voids. In the case of simple structures, such as disks fully embedded between the sheets of LTCC, the standard lamination process can be applied according to datasheet guidance. However, when manufacturing complex 3D structures, lamination should be carried out with special care, preferably in several steps as shown in Fig.7.

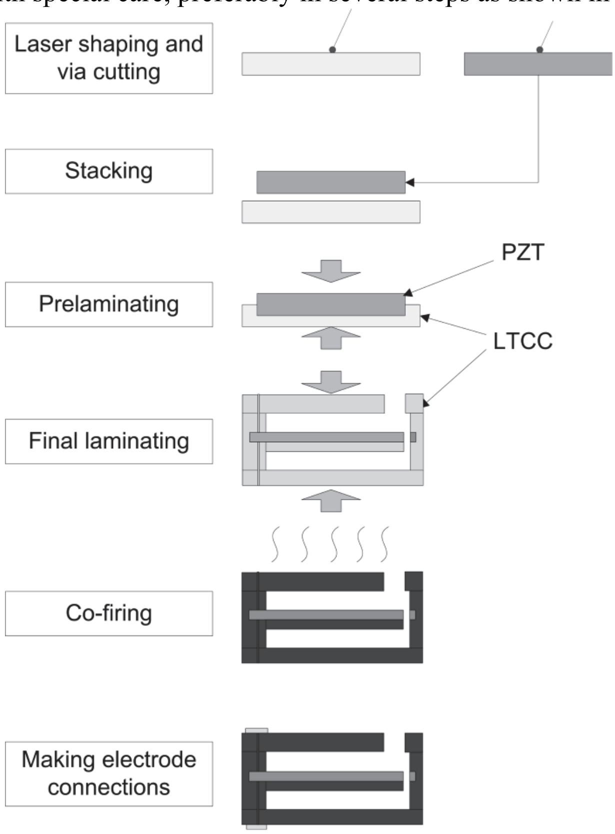

Fig. 7. Modified LTCC process flow includes multiphase lamination, which ensures a good connection between LTCC and PZT as well as a undisturbed 3D form for the package (Paper II). Reprinted with the permission of Elsevier.

The two-step lamination procedure proposed in the Paper II should be carried out as follows. First, the piezoelectric component has to be laminated with the tapes being in direct contact with the bottom of the structure and its sides, using a uniaxial press with heated surfaces. This will ensure no delaminations between the piezoelectric structure and LTCC. Care has to be taken in precise positioning, as misalignment might cause cracks in the stiff piezoelectric bulk structure. Furthermore, it has been noted that silicone rubber inserts in cavities might also cause cracks in the piezoelectric bulk when the laminating pressure is being transferred to the edge of the bulk structure. Temperature and pressure described in the HeraLock 2000 datasheet can be used; however, it is beneficial to extend the time of lamination to 20 minutes in order to facilitate better connection between the unsintered LTCC and the bulk piece. Dwell time before applying pressure is also important, as time should be given for the LTCC to warm up and soften. Other parts of the structure should be laminated separately, no changes in profile necessary, and finally, all parts should be laminated using the 20-minute time in the uniaxial press. Subsequently laminated structures are ready to be sintered in the temperature profile indicated by HeraLock 2000 datasheet.

Sintering at the elevated temperature causes the LTCC to densify and softens the thick-film silver electrodes present on both sides of PZT. The softened electrode acts as adhesive forming a strong connection between the two ceramics while still ensuring electrical connection to the piezoelectric material. The brazing bond ensures good, stable adhesion, high reliability and hermetic packaging. Furthermore, it allows the structure to work in temperatures that would be harmful for adhesives. In structures where the piezoelectric element had thin-film electrodes or did not have electrodes at all the bonding between the two ceramics was of lower quality. A cross-section through an LTCC-PZT multilayer from Paper I is presented in Fig. 8. The left side of the figure presents an excellent connection between the ceramics; however, on the right side a gap can be noticed at the edge of the bulk PZT, which was created during lamination, and might lead to reliability issues. In order to avoid those issues the co-fired structures presented in Papers II, III and IV had tailored cavities for the bulk PZT elements that ensured tight fitting and minimized the gap at the edge.

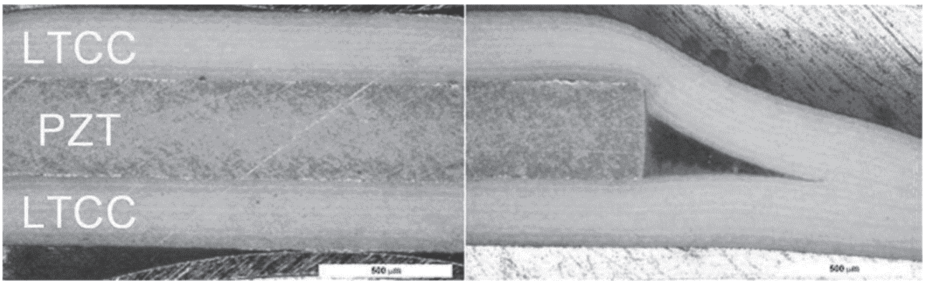

Fig. 8. A cross-section of the LTCC multilayer with embedded PZT disk. The thick film electrode of the PZT forms an excellent seamless adhesive layer between the ceramics, ensuring high durability of the connection and hermitic packaging. The gap in the corner is formed when PZT disk is placed between LTCC without preparing tailored cavity (Paper I). Reprinted with the permission of Maney Publishing.

In case of not non-shrinkage tapes, such as DuPont 951, the large planar shrinkage bends the bulk structures as shown by Juuti *et al.* (2006). Given a fully embedded structure, such large distortion would lead to LTCC warping, cracks and general destruction of the sample. Similar effects were observed when embedding other materials e.g. optical fibres in DuPont (Kara, 2004).

After sintering, the piezoelectric structure embedded inside the LTCC needs to be poled, since the sintering temperature of the LTCC multilayer is above the Curie temperature of most piezoelectric materials, resulting in depolarization and loss of piezoelectric properties. In poling the domains in the piezoelectric ceramic turn along the direction of applied electric field. The more domains arranged along the poling direction, the higher the remnant polarization and the better the piezoelectric properties. Furthermore, elevating the temperature in which the poling takes place makes the domains switch much more easily, therefore lower electric fields are required. The poling temperature for most of the samples was 125 °C. Optimum poling conditions can be studied using the Radiant hysteresis measuring setup by investigating the values of remnant polarization and comparing it to bulk bare sample (Juuti *et al.* 2005).

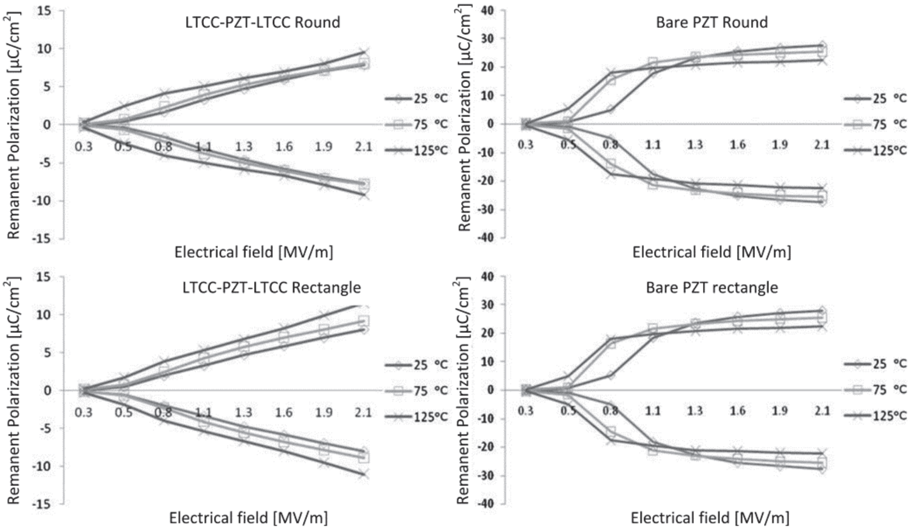

Fig. 9. Remanent polarization in the function of electric field for LTCC embedded samples and reference bulk PZT samples. Remanent polarization gives good approximation of a structure's performance after poling; therefore, it is desirable to achieve the highest possible P_R after which saturation occurs as seen in the reference samples (Paper I). Reprinted with the permission of Maney Publishing.

Fig. 9 shows that in the case of bare PZT structures the remnant polarization tends to saturate after a 0.8 kV/mm field is applied at the temperature of 125 °C; this signals that most of the domains are aligned. In the case of an LTCC embedded structure, the saturation does not occur even when reaching 2.1 kV/mm at 125 °C (after which electrical breakdown of the PZT happened). The conclusion is that fields and temperatures used in poling the structures presented in Paper I were not high enough to restore polarization to the level before co-firing. This of course influences the piezoelectric properties lowering them significantly. In fact, samples presented in Paper I obtained only about 30% of the remnant polarization measured for the bare sample. One of the reasons behind the lower quality of poling might be the stress generated by the mismatch of temperature coefficients of PZT and LTCC and the mechanical constraint of the piezoelectric part. Wang *et al.* (1989) and Juuti *at al.* (2005) have shown that prestressed samples require higher fields for optimal poling.

Even though poling conditions have not been yet optimized, integrated bulk piezoelectric structures have shown improved performance compared to thick-film ones due to generally higher piezoelectric properties and lower influence of diffusion during co-firing. Closer comparison can be found in following chapter.

4 Applications of PZT-LTCC structures

Three different PZT-LTCC structures were manufactured using the co-firing method and one structure was manufactured using post-firing adhesive attachment. Each structure addressed one of the main areas where the integration of bulk PZT with LTCC would bring significant benefits. Examples of a sensor, actuator and energy harvester were manufactured by co-firing, and a meso-scale valve was assembled by adhesive bonding. In each case results of manufacturing were satisfying. Structures were crack free and no delaminations were observed. There were no problems handling the structures either before or after sintering. Their robustness and resistance to shock was noteworthy. Furthermore, thanks to the large size of LTCC tapes, it was possible to manufacture more than one sample at the same time, indicating the feasibility of the methods for mass production.

4.1 Actuators

In the area of actuators, piezoelectric materials offer incredible nanometer precision of displacements. For this reason, they are widely used in all kinds of moving stages, for aligning optics, lasers and adjusting resonator chambers. Park & Shrout (1997) report the typical strain induced in PZT materials lies in the area of 0.1% - 0.2%. Assuming thicknesses ranging from 100 µm to 500 µm, performance of single plate actuators might be therefore rather limited. However, it is possible to employ one of the few methods of enchasing displacement in case larger displacements are needed.

One of the easiest ways to amplify the displacement of actuators, presented by Takahashi *et al.* (1983), is to use a stack of piezoelectric plates. Stacked actuators consist of many piezoelectric plates placed one on another and electrically connected, so even though one plate produces only one µm of displacement, a stack of 100 of them will produce 100 µm. The benefits of stack actuators are low operating voltage, quick response, and high generated force. Furthermore, stack actuators can be produced using multilayer ceramic technology known from capacitor manufacturing, making them cheap and widely available (Uchino 2000).

Another way to enhance displacement is to force the piezoceramic plate to bend. Bimorphs, unimorphs and monomorphs are structures usually made of two materials acting against each other in order to generate bending type displacement. Germano (1971) and Niezrecki *et al.* (2001) give a good review on the subject. In bimorph actuators, two piezoelectric plates poled in opposite directions are joined together, and while one is expanding under applied voltage, the other one is contracting. The difference in the direction of dimensional change causes the whole structure to bend. In unimorph actuators, the constraining role is given to a passive layer – steel, brass or other non-piezoelectric material - which constrains the piezoelectric plate and causes the bending motion. Monomorph actuators have a similar principle of operation. However, the passive layer is induced in the piezoelectric material itself through reduction, doping or co-firing rather than by bonding with adhesive. Bending actuators provide large displacements at the cost of low force and relatively long response time of about 1 ms.

Finally, the displacement can be enhanced through a lever device such as a moonie or cymbal actuator. Presented first by Sugawara *et al.* (1992) and Dogan *et al.* (1996) respectively, these externally levered actuators are characterized by a piezoelectric plate placed between two metal caps with a moon or cymbal shaped cavity in between. In these configurations, the radial displacement of the piezoceramic causes the metal plates to bend out along the axis perpendicular to the surface. Moonie and cymbal actuators offer a compromise between the fast response and large force of stack actuator and the large displacement of benders. (Uchino 2000)

The ultrasonic motor is an interesting actuator. A typical design consists of a piezoelectric stator and non-piezoelectric rotor. The stator can work in one of two ways. In the first design, the stator generates a travelling wave on which the rotor "surfs" from one place to another. In the second design, the stator generates a "pecker-like" motion displacing the stator by nanometers every time it encounters the rotor. Ultrasonic motors have several advantages over electromagnetic ones, especially when scaled down to few millimetres. They have quick response, high torque and a wide velocity range, present an excellent weight to power ratio and produce no noise in the audible range. Furthermore, they are relatively easy to manufacture, especially in small sizes. Among their applications are autofocus systems in cameras (Canon 2012), watches (Seiko Instruments Inc. 2013), rear-view car mirrors, in-vitro fertilization equipment and many others (Chunsheng 2011). Dong *et al.* (2003) presented a version of the ultrasonic motor configured as follows. A 1.5 mm thick piezoelectric tube had four separate electrodes manufactured on the outside and one common electrode on the inside. By driving the outer electrodes with appropriate signals, a rotary motion of the middle part was acquired.

In this thesis, an actuator with three arms for circular mirror suspension was manufactured to be used in portable Fabry-Perot interferometers. A photo of an actual structure used can be seen in Fig. 10 and a schematic cross-section through the structure can be seen in Fig. 11.

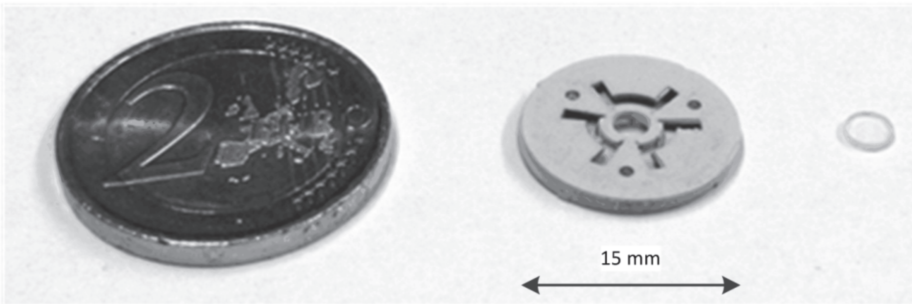

Fig. 10. An example of a monomorph actuator designed for a portable Fabry-Perot interferometer. The three bending arms provided the ability to move the small mirror in two axes allowing levelling of the mirror by tilting up to 0.06° and changing output wavelength by up to 680 nm (Paper III). Reprinted with the permission of IEEE.

In this case, the LTCC acted as a package, mirror support, and passive layer forming PZT-LTCC monomorph, which greatly enhances the displacement compared to bare bulk devices. The whole structure with the package had a diameter of 15 mm and a thickness of 1.8 mm. The PZT structure cut out from a single PZT disc had three electrically independent areas established with laser trimming and was embedded in LTCC on all sides. The 2.9 mm tapered arms were connected with LTCC support for an inner 4 mm wide mirror. The second mirror, needed for the operation of Fabre-Perot interferometer, was meant to be mounted on the outside, distanced by several layers of LTCC forming a resonator chamber. It was planned the mirrors would be assembled after sintering, and the gap between the mirrors would be set by changing the number of LTCC tapes between the mirrors.

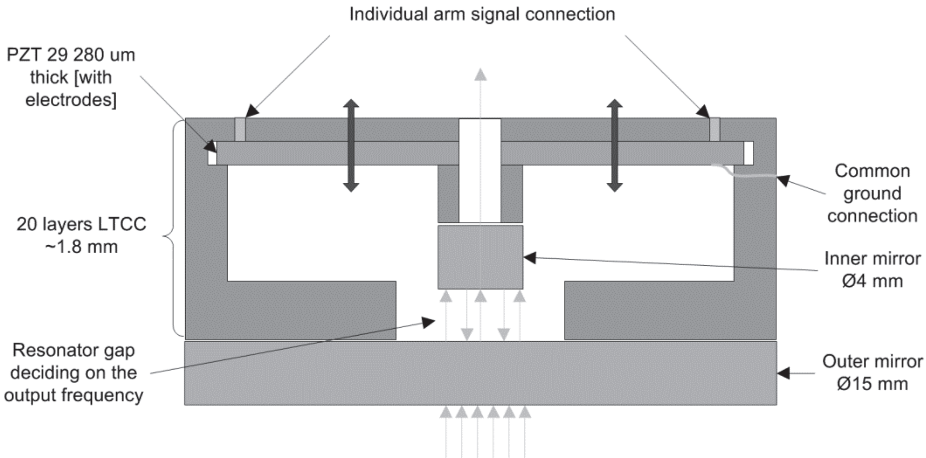

Fig. 11. Schematic representation of LTCC-PZT Fabry-Perot interferometer module. The LTCC acts as passive layer causing the PZT arms to bend rather than elongate, as a holder and distancer for the mirrors, and as a package for the whole structure (Modified from Paper III). Reprinted with the permission of IEEE.

Tests which included the usage of laser Doppler vibrometer (OFV-5000, Polytec GmbH, Germany) showed the frequency characteristic of the structure, maximum displacement of the centre of the mirror and stabilization time. During the operation, the gap could be furthermore changed in the range of 680 nm by applying voltage to the arms, which result would displace the inner mirror and change the output frequency of the interferometer. Moreover, the three independent arms provide 0.06° tilt allowing the levelling of the mirror surfaces, which is important for the interferometer operation.

The application of piezoelectric ceramic in a form of bending actuator provided large displacements with relatively low voltage and a fast switching time, which theoretically would allow this structure to change its output wavelength with the frequency of 588 Hz. A comparison to other interferometer structures is presented in Table 2. The LTCC-PZT Fabry-Perot interferometer had compact size being larger only compared to a MEMS based structure (Patterson, 1997), and response 10 to 1000 times faster than other reported in (Atherton and Reay, 1981) and (Yu *et al*, 2004) respectively. Furthermore, the driving voltage was smaller than other piezoelectric solutions presented by (Reay *et al*, 1974) and (Atherton and Reay, 1981).

Integrating the piezoelectric element with the LTCC package at the co-firing level increased the structures reliability by eliminating adhesive mounting and wire connections used in traditional packaging. Furthermore, large size of the LTCC substrate allowed parallel processing of five structures at the same time (Fig. 6). The LTCC package proved to be a durable protection as well as stable platform for mounting the mirrors.

Table 2. Comparison of PZT-LTCC module to other structures (Modified from Paper III). Reprinted with permission of IEEE

	Dimensions [mm]	Displacement [nm]	Operating wavelength [nm]	Resonance frequency [kHz]	Switching time [ms]	Operating voltage [V]
PZT-LTCC	diameter 15 x 1.8	600	200 to 800	11	1.7	100
Piezo stack[1]	150 x 110 x50	120	440 to 560	-	-	1000
Piezo stack[2]	diameter 85	6700	430 to 640	-	20	800
Thermal[3]	32 x 95 x 140	90.8	1459 to 1640	-	~2000	2
Electrostatic[4]	0.25 x 0.40	3200	700 to 900	57	-	53

1. Reay *et al*, (1974)
2. Atherton and Reay, (1981)
3. Yu *et al*, (2004)
4. Patterson (1997)

4.2 Energy harvesters

The ongoing miniaturization of electronics decreases their need for power. It has been proposed recently to power these small devices with energy recovered from our surroundings, such as human motion, structure vibration or pressure. Taking into consideration the fact that the piezoelectric effect is one of best ways to transduce mechanical energy to electrical energy, many designs of piezoelectric energy harvesters have been proposed. IDTechEx forecast that the market for piezoelectric energy harvesters will grow to $145 million by the year 2018 (Das 2012). Designs ranging from vibration based systems, through impact harvesters in the soles of our shoes (Howells 2009) up to piezoelectric leafs (Li *et al.* 2009) have been proposed.

Paper II presents a 39 mm x 39 mm structure with the thickness of 2.7 mm containing three beams of different lengths (18 mm, 17.78 mm, 17.56 mm) cut out from a single 375 μm thick 25 mm in diameter PZT disk, laminated with LTCC packaging, co-fired and electrically poled. A schematic overview of the structure is shown in Fig. 12 and a photo in Fig. 13. Again, the LTCC acts as packaging and a passive layer for the monomorphic piezoelectric structure.

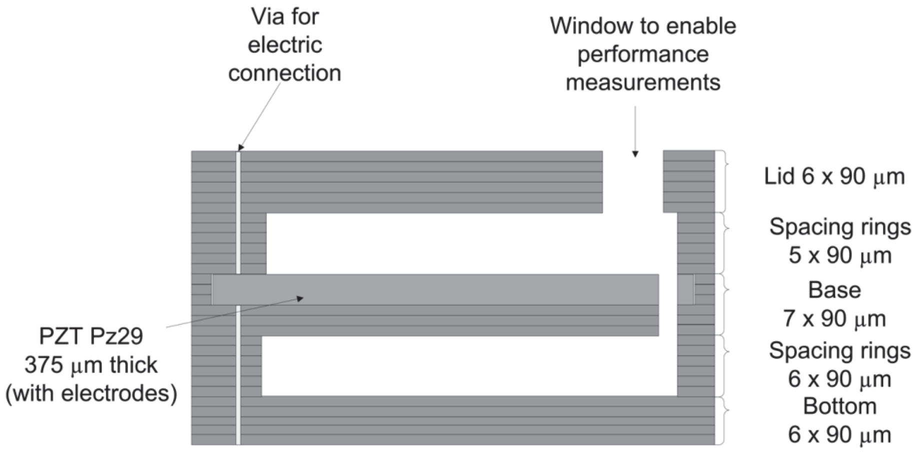

Fig. 12. Schematic cross-section of a packaged energy harvester. Similar to the interferometer structure, LTCC acts here as the passive layer for the PZT and as a package for the whole structure. The three-beam setup gives the device a broadband behaviour with 5.4% bandwidth and the maximum output power to a matched resistor of 85 μW (Paper II). Reprinted with permission of Elsevier.

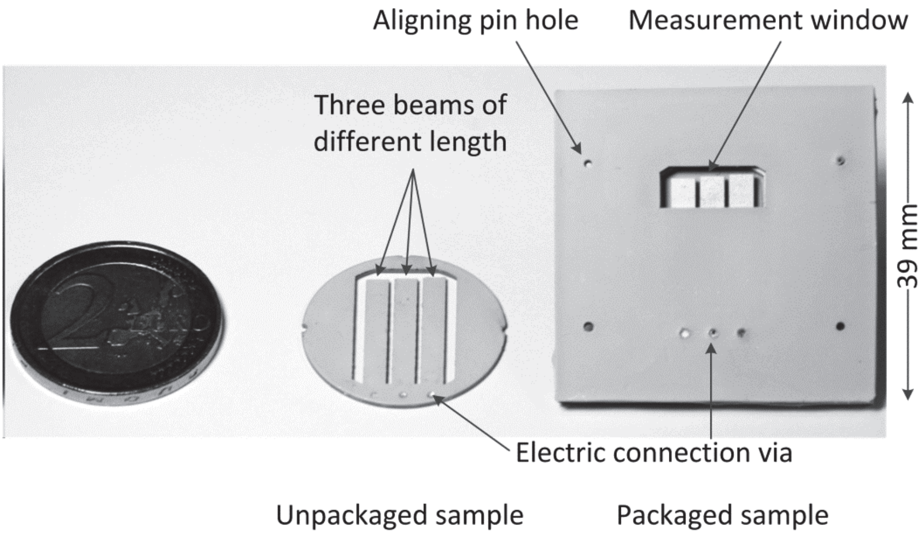

Fig. 13. Photo of the unpackaged and packaged harvester structure compared to a 2 Euro coin. The packaged structure exhibited improved performance compared to the bare monomorph due to larger stiffness and better mechanical isolation of each beam. Bandwidth was doubled and generated power tripled (Modified from Paper II). Reprinted with permission of Elsevier.

The three-beam approach broadens the frequency bandwidth of the harvester allowing better performance compared to a single beam structure in the terms of frequency span and generated power.

A comparison between packaged and unpackaged structures has also been carried out. The existence of the package not only shielded the structure from external environment but also improved its overall performance. The higher stiffness of the package increased the mechanical isolation between the beams, boosting the bandwidth two times and the output power three times. It has also slightly higher centre frequency by about 70 Hz. The complete comparison between a packaged and an unpackaged sample can be seen in Table 3.

Table 3. Summarised performance of reference and packaged harvesters (Paper II). Reprinted with permission of Elseiver.

Sample	No package	Package
Centre Frequency [Hz]	1076	1147
Bandwidth [%]	2.7	5.4
Voltage output [V]	4.7	5.6
Total generated power [μW]	25.9	85.0
Power output per 1g of acceleration [$\mu W g^{-1}$]	11.5	32.0
Power density per area of piezo [$\mu W g^{-1} cm^{-2}$]	7.2	20.0

The LTCC embedded harvester exhibited excellent output power reaching 85 μW with matched resistive load and the three beams of varying length allowed wideband frequency behaviour with 5.4% bandwidth around the centre frequency of 1147 Hz. A graphical representation of results is presented in Fig. 14.

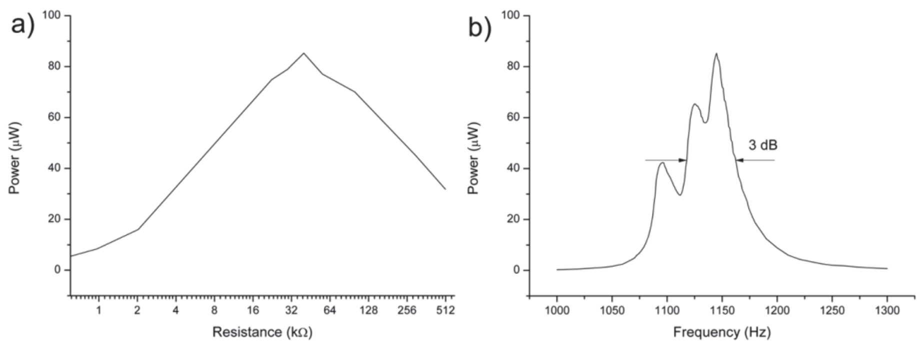

Fig. 14. (a) Power generated by packaged structure as a function of different loads. (b) Overall power generated by three beams of the packaged sample as a function of frequency with 39.9 kΩ resistive load (Paper II). Reprinted with permission of Elsevier.

The generated energy would be sufficient to power for example a LM19 temperature sensor, a LIS3DH accelerometer or a ZigBit 900 Wi-Fi module operating in data burst mode. The hermetic package can make it resistant to environmental conditions, which would make it a perfect solution for distributed sensor networks. The generated power was 200 times higher compared to Sari *et al.* (2008), 4 times higher compared to the open package structure reported by Elfrink *et al.* (2009) and 1000 times larger compared to a single layer thick-film approach presented by Kok *et al.* (2009). A 17.5% bandwidth was reported by Sari *et al.* (2008) which is about 3 times larger than the one presented in Paper II, however the better performing structure had over 10 times more beams which complicates manufacturing and handling. The performance of the harvester presented in Paper II can be easily tuned at the designing stage to match the requirements of application through careful selection and design of the piezoelectric material and length of the beams.

4.3 Sensors

In the area of sensors, one of the most basic application employing the direct piezoelectric effect is the pressure sensor. Pressure sensors come in different sizes and different packages. They are designed for different operating temperature and pressure ranges. They can be used to measure pressure changes in both liquids and gases. Some of the vendors supplying piezoelectric pressure sensors are A-tech Instruments Ltd, Meggit PLC and Thermo Fisher Scientific.

Microbalances are a special kind of pressure sensors. Their operation principle (as presented, for example, by Spetz (2006)) is based on changes in resonance frequency due to mass gathered by the selective binding layer. First presented by King (1964), Quartz Micro Balances (QMB) were designed as simple gas sensors. Nowadays, more and more of them are used in the detection of pathogens, viruses and bacteria as shown by Mulder (1984) and Prusak-Sochaczewski *et al.* (1990). The sensitivity of such devices can reach a few ng/cm^2. A radical application of microbalances presented by Wu (1999) and Zampetti *et al.* (2008) is the electronic nose/tongue, which consists of several microbalances each sensitive to a different aromatic molecule.

Another type of piezoelectric sensor is the SAW sensor, presented first by Wohltjen & Dessy (1979) and Bryant *et al.* (1982), where a set of interdigital electrodes generates a surface travelling wave that is disturbed by the mass adsorbed by a chemically interactive layer placed on the path of the wave. Another set of electrodes receives the disturbed wave and measures the changes in velocity, amplitude or frequency. SAW sensors are now often used for the detection of gases, including warfare agents, and can also be arranged in an array for multipurpose use as shown by Lim *et al.* (2011) and Matatagui *et al.* (2011).

In 1943, Brüel & Kjær (Sound and Vibration Measurement A/S) introduced another type of widely used piezoelectric sensor to the market - the acceleration sensor. The operation principle of this sensor is usually based on seismic mass stressing the piezoelectric element during changes in acceleration. Piezoelectric accelerometers are characterized by their wide dynamic range, excellent linearity and wide frequency range. Furthermore, limited movement of the sensing element, its high mechanical strength and compact size makes the piezoelectric accelerometer excellent for harsh working conditions (Wagner & Burgemeister 2012). Piezoelectric accelerometers are widely available from vendors such as Meggit PLC and Brüel & Kjær (Sound and Vibration Measurement A/S).

In the area of sensors, a simple seismic mass based accelerometer is presented in Paper IV. PZT material is laser cut into the desired shape, laminated and co-fired with a 15 mm x 15 mm LTCC package with the thickness of 2.16 mm. The LTCC provides a stable frame for the PZT sensing element, as well as offers possibilities for electrical connections and hermetic encapsulation. For ease of measurement, the LTCC package presented here was left open. After sintering the structure has been electrically poled in a silicon oil bath with 2.4 V/µm electric field. A schematic cross-section of the structure is presented in Fig. 15 and a photo in Fig. 16.

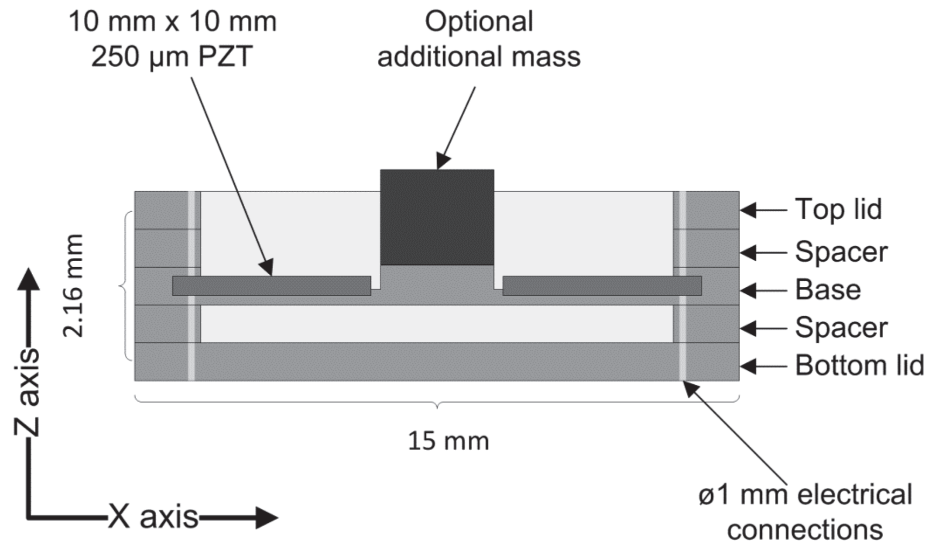

Fig. 15. A schematic cross-section through accelerometer structure constructed from two PZT arms cut from one disc, LTCC mass support attached to the arms with a hinge-like structure and LTCC packaging with suitable electrical connections (Modified from Paper IV). Reprinted with permission of Elsevier.

The PZT-LTCC structure consisted of laser shaped single 10 mm x 10 mm pieces of PZT 250 µm thick with two arms and a thin frame embedded in 24-layer LTCC packaging. The sensing arms of the structure were connected together by the LTCC mass supported by 180 µm thick hinge-like structures which proved to have no problems supporting up to 71 mg of additional mass even at 50 g acceleration. Employing two arms connected by flexible joints ensured the possibility of large displacements of the mass, maintaining high robustness and insensitivity to in-plane accelerations. The LTCC layer in direct contact with PZT acted also as a pre-stressing layer, forming a monomorph structure. The higher stiffness of the structure compared to a bare bulk material and slight curl of the arms shifted the resonance frequency towards higher values compared to bare bulk solution. The curl resulted from the shrinkage of the LTCC and CTE mismatch and most probably occurred also in structures from Paper II and III. This effect can be reduced by choosing the right combination of LTCC and piezoelectric material, minimizing the difference in CTE. Manufactured structures had their resonance frequency determined and output signal as a function of acceleration measured. The structures were submitted to accelerations from 5 g to 50 g which upper limit was limited by the measuring system.

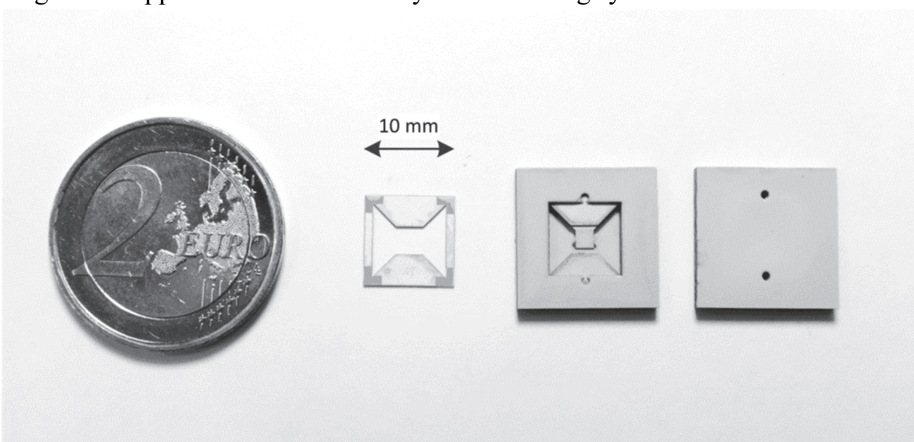

Fig. 16. A photo of the 10 mm x 10 mm PZT sensing element, 15 mm x 15 mm measured structure, and proposed packaged sample, compared to 2-euro coin. An opening in the top lid has been left in the measured structure for ease of measurements. Sensitivity up to 6.13 mV/g was measured with 90% lower sensitivity to in-plane displacements (Modified from Paper IV). Reprinted with permission of Elsevier.

The measurements were performed for structures with and without additional mass using a mini-shaker (Type 4810 by Brüel & Kjær, Denmark), laser vibrometer (Polytec OFV-552, Germany) and oscilloscope (Tektronix TDS2024B, UK). The results are presented in Fig. 17. Sensitivity up to 6.13

mV/g was measured for the structure with additional mass and the resonance frequency was at the level of 12.1 kHz. Calculated useful bandwidth of operation spanned up to 7.5 kHz above which the output signal increased by more than 10%. High linearity was obtained reaching the coefficient of determination R^2 of 0.9962 and 0.9930 for each of the beams without additional load. The mass addition improved the R^2 values slightly to 0.9983 and 0.9994 respectively.

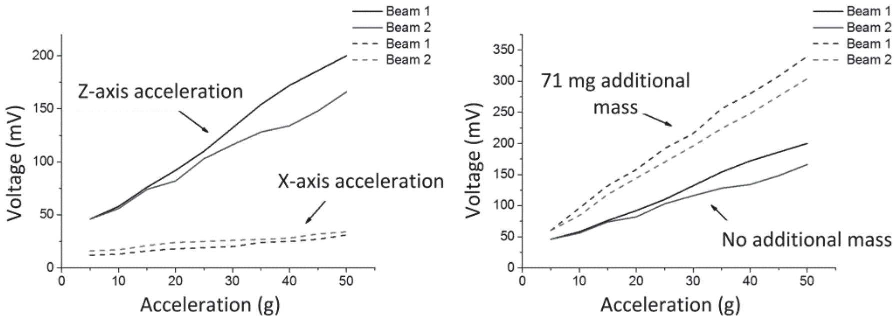

Fig. 17. Sensitivity of the PZT-LTCC accelerometer. a) In different directions; b) In z-axis with and without 71 mg mass. Though additional mass greatly improves the sensitivity, it also lowers the resonance frequency limiting the bandwidth of the device (Paper IV). Beam 1 and 2 refer to the arms of the accelerometer (Paper IV). Reprinted with permission of Elsevier.

A certain discrepancy between the arms has been noticed, which might be the result of the additional mass not being placed exactly in the middle. It has been also noticed that the discrepancy is dependent on the increase of seismic mass due to larger stresses imposed on the beams. Measurements with in-plane accelerations were made for the structure without additional mass, showing sensitivity lower by 90% compared to the direction for which it was designed. Compared to other non-commercial structures such as reported by Jurkow et al (2013), Hindrichsen et al (2009) and Hindrichsen et al (2010) the loaded structure showed at least ten times higher sensitivity with similar frequency range and dimensions. Compared to commercial solutions of similar size employing piezoresistive effect (Endevco b, 2012) (Endevco c, 2012) this structure showed an order of magnitude higher sensitivity with similar resonance frequency. Commercially available capacitive accelerometers (Kistler, 2012) (Silicon Designs, 2012) exhibited 3 to 7 times higher sensitivity but also about 5 times narrower frequency span. The structure was also comparable to some commercially available piezoelectric accelerometers such as those presented by

(Metra Mess- und Frequenzrechnik in Radebeul e.K. 2012) and (Endevco a, 2012) even though no amplification was present. A more detailed comparison can be seen in Table 4.

Table 4. Summarized comparison of structure presented in Paper IV and other accelerometers (Modified from Paper IV).Reprinted with permission of Elsevier.

Reference	Type of sensor	Sensitivity	Resonance frequency [kHz]	Frequency range [Hz]	Dimensions [mm]
This paper	piezoelectric embedded bulk	z: 6 mV/g- with additional mass	12.1	1-7500	15x15x2.16
		z: 3.6 mV/g without additional mass	32.7	1-23500	
[1]	piezoelectric thick-film	0.28 pC/g	>6	4800-6000	approx. 15x15x2
[2]	piezoelectric thick-film	0.24 mV/g	23.5	100-4000	10x10x0.5
[3]	piezoelectric thick-film	x&y:0.062 mV/g z: 0.31 mV/g	x&y: 23 z: 11		3.6x3.6x0.05
[4]	piezoelectric commercial	10 * mV/g	42	0.2-22000	22.5x20x 11.2
[5]	piezoelectric commercial	100* mV/g	9	0.25-3000	10x10x10
[6]	piezoelectric commercial	10* mV/g	20		15.04x15.04x18.67
[7]	piezoresistive commercial	0.15*mV/g	14		19.05x19.05x22.86
[8]	piezoresistive commercial	0.80*mV/g	17	z: 0-3000 x&y: 0-1500	10.67x13.04x 12.70
[9]	capacitive commercial	40 mV/g	7.2	0-1000	21.59x21.59x22.10
[10]	capacitive commercial	20* mV/g		0-3000	25 x 25 x21

* structure has internal amplifier

1. Jurkow *et al* (2013)
2. Hindrichsen *et al* (2009)
3. Hindrichsen *et al* (2010)
4. Metra Mess- und Frequenzrechnik in Radebeul e.K. (2012)
5. Brüel & Kjær (2012)
6. Endevco a (2012)
7. Endevco b,(2012)
8. Endevco c (2012)
9. Kistler (2012)
10. Silicon Designs (2012)

The robust LTCC package with the possibility of manufacturing the amplification system on the top creates an opportunity for inexpensive, reliable, surface mountable accelerators suitable for both everyday use and extreme conditions.

4.4 Microfluidic meso-systems.

Both PZT bulk structures and LTCC are being used separately in the manufacturing of various microfluidic systems in the meso-scale. From the LTCC point of view, the first Micro Total Analysis System (μTAS) structures were presented by Gongora-Rubio *et al.* (2001). Since then, more approaches to manufacture microfluidic chips on LTCC have been taken such as those described by Gongora-Rubio *et al.* (2004), Golonka *et al.* (2005), Malecha *et al.* (2009) Barlow *et al.* (2009) . However, none of the structures presented had a working valve. On the other hand, PZT bulk actuators are already used to manufacture structures such as pumps (Yang *et al.* *(*2005), Hayamizu *et al.* *(*2003), Peng & Zeng (2009)) and valves (Hirooka *et al.* (2009), Yun *et al.* (2006)) on different substrates.

The design for the piezoelectric valve used here includes a moving membrane operated by a piezoelectric element, which in the valve off state presses against valve's seat. An example of such a structure can be seen in Fig. 18.

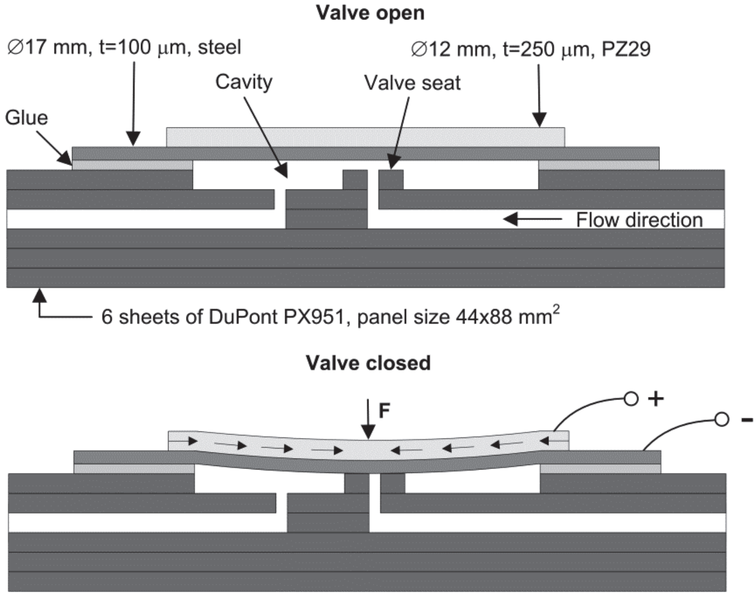

Fig. 18. A schematic cross-section t of LTCC-PZT valve, explaining the working principle. The thick bottom layer of LTCC was chosen as a base for the LTCC on which channels have been fabricated. The inlet and outlet within the valve seat were placed so that the inlet would be directly under the centre of the moving membrane for better sealing capabilities (Paper V). Reprinted with permission of Elsevier.

The distance that the membrane can travel is determined by the performance of the piezoelectric element, and considering size limitations for microfluidics devices, would not be greater than a few micrometres. In LTCC preparation, the process of creating controlled gaps between the LTCC structures can be done either by cutting the tape and forming a cavity or by utilizing sacrificial volume material that burns out completely during the burn out phase of LTCC sintering. In the first case, the distance between the two tapes depends on the tape's thickness and varies from 50 μm to 250 μm (in the "green" state). In the second approach the gap can be made thinner by using screen printed Sacrificial Volume Material (SVM) paste. Using standard thick film technology a gap of around 10 μm can be manufactured. Therefore, in order to close the piezoelectric valve manufactured using the co-firing method presented earlier, one would need to generate 10 μm of displacement, which translates to a large size for the actuator and a large driving field, not necessary welcomed in microfluidics devices.

An obvious solution to keep the piezoelectric actuator small is to minimize the gap that the membrane needs to travel in order to close the valve. One of the ways to do that is to emboss the membrane. If the membrane is made out of LTCC, embossing it in the "green" state would cause permanent lamination, and no displacement could be obtained whatsoever, while trying to emboss it after sintering would result in crushing of the ceramic. Therefore, in this case embedding through co-firing could not be used.

Instead, the piezoelectric actuator and the membrane can be mounted on the LTCC substrate in the post-processing step by adhesive bonding using the following method. After preparing the substrate with microchannels and the valve seat, a thin sheet of steel was mounted on top of the valve seat to act as a moving membrane. Common cyanoacrylic glue was used for the assembly and carefully applied at the rim of the membrane. Next, embossing was performed using a uniaxial press with soft silicon pad on the top of the structure. The elastic pad will distribute the pressure across the steel membrane, pushing it towards the bottom of the valve seat. Due to the plasticity of the steel membrane, the embossed shape will stay even when the pressure is taken away. This minimized the traveling distance for the membrane making it possible to use smaller piezoelectric actuators. Additionally, embossing flattened down any irregularity in assembly caused by uneven glue distribution. Finally, the piezoelectric element was mounted by bonding with adhesive and electrical connections were made. A valve assembled in this way is presented in Paper V and its photograph can be seen in Fig. 5 and schematic view of the valve seat is shown in Fig 19.

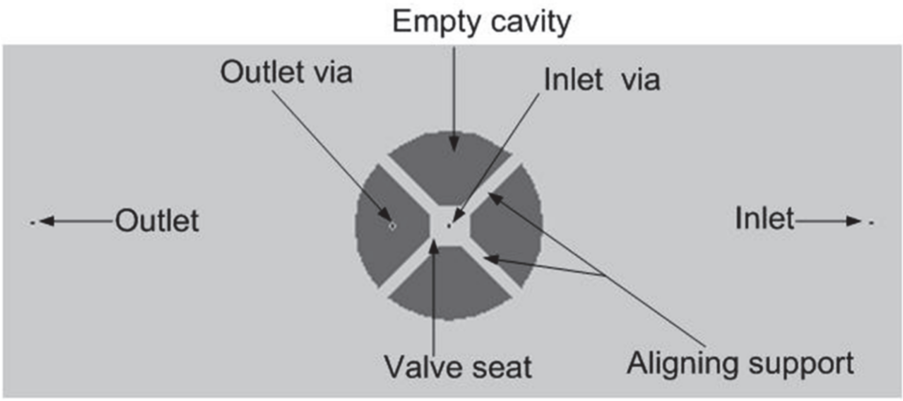

Fig. 19. Top view of LTCC valve seat. The somewhat complicated design of the valve seats has twofold purpose. On one hand, it provides empty space for excess of glue that holds the unimorph actuator and on the other, it allows the steel membrane to close off the valve more efficiently through embossing (Paper V). Reprinted with permission of Elsevier.

The performance of the valve is rather modest in the respect of size and leakage when compared to silicon based Micro Electro Mechanical Systems (MEMS) structures. The valve presented in Paper V exhibited 4% leakage when closed due to LTCCs surface roughness, which is two orders higher than silicone's. However, the closing times presented in Fig. 20 were quite promising. Furthermore, it has been proven that it is possible to manufacture a piezoelectric valve on LTCC substrate. In meso-scale applications it could be used to govern the flow rate. Future studies could include research on lowering of the leakage through polishing of the substrate or using softer membrane; and new ways of integration.

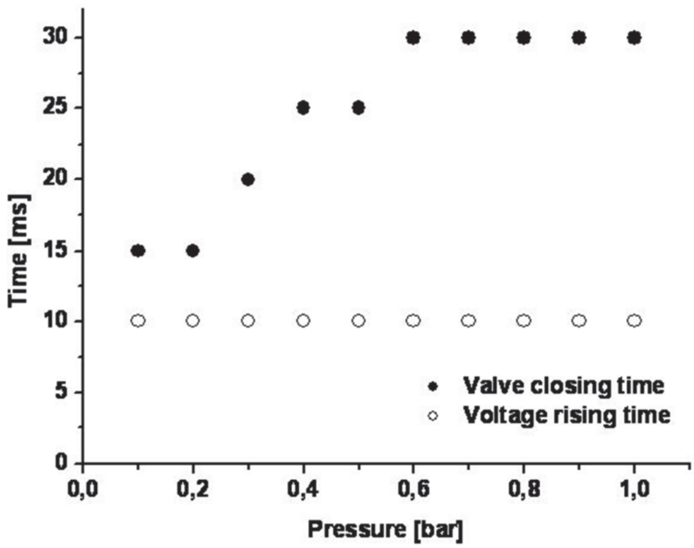

Fig. 20. Closing times of the LTCC-PZT valve. One of the benefits of the piezoelectric unimorph valve is its fast reaction time to applied voltage and the high force it applies (Paper V). Reprinted with permission of Elsevier.

5 Conclusions

The focus of this thesis is the integration of piezoelectric bulk structures in LTCC. The thesis presents bonding with adhesive and co-firing as methods for assembling PZT-LTCC structures. Four different structures have been manufactured using commercially available materials: Heraeus HeraLock 2000 LTCC, DuPont 951 LTCC and Ferroperm Pz29 piezoelectric disks with thick-film silver electrodes. Performance of the integrated structures has been investigated and benefits and drawbacks of both methods concluded. Each investigation presented a novel, previously not available structure from the main areas of piezoelectric applications.

Investigation of the co-firing method showed that by making small modifications to the LTCC manufacturing process it is possible to produce reliable structures with piezoelectric properties. Structures manufactured by co-firing presented excellent durability, ease of handling and performance similar or better to structures manufactured using other techniques. Piezoelectric components can be co-fired in closed, hermetic packages, which offer excellent protection from the environment. Bonding allows the structures to work in higher temperatures, provides excellent aligning, and no contamination of the adjacent surfaces. LTCC thick-film conductive pastes can provide electrical connections to the piezoelectric component and circuitry needed for preconditioning of the signal. Using bulk piezoelectric materials in combination with LTCC brings many benefits compared to thick or thin film methods. Bulk structures offer better performance in the term of higher piezoelectric coefficients. They are also less sensitive to diffusion and do not need a barrier layer which is the main issue with thick film piezoelectric materials. Bulk piezoelectric structures adhere very well through the thick-film electrode to the surface of LTCC which is usually too rough for direct thin-film deposition and they do not require vacuum environment for embedding. On the other side, co-firing nullifies the alignment of piezoelectric domains inside the bulk structure creating the need for additional manufacturing step – poling. This step is responsible for the piezoelectric performance of the LTCC-piezoelectric structure and needs to be further studied in order to pinpoint the optimal conditions so the final properties could be maximized.

System-in-Package solutions can be obtained and surface mounted to PCB through flip-chip bonding. Components made through co-firing can be easily trimmed to meet the needs of resonance frequencies, output voltage, driving field, displacement, and so on by changing the design or by changing the bulk piezoelectric materials used including lead-free solutions. Furthermore, by using piezoelectric materials with high Curie temperatures, post-processing poling might be excluded which would result in better performance and the possibility to use the structures in elevated temperatures.

On the very few occasions when co-firing shows its limitations, bonding with adhesive can be used as the binding medium between the bulk piezoelectric component and LTCC. Though the bond produced will not be as durable as the co-fired bond, certain benefits can be obtained. First, adhesive bonding does not require elevated temperatures, therefore no depolarization occurs which means the piezoelectric component will have its original properties. Furthermore, there is no need to modify any of the steps of LTCC manufacturing, and finally, in applications such as valves, narrow gaps between the membrane and the valve seat can be obtained through embossing.

With ongoing development of electronics and need for autonomous, wirelessly controlled devices integrated sensors, actuators and energy harvesters is very high. LTCC technology is important part of modern packaging; together with piezoelectric elements is represents the best solution for the industry’s needs. The integration methods presented in this work deliver robust and reliable structures and are available for immediate implementation in industry, using existing production lines offering relatively inexpensive, mass produced Systems-in-Package, ready to be surface mounted by flip-chip technology or other means.

References

Atherton P and Reay N (1981) A narrow gap, servo-controlled tunable Fabry–Perot filter for astronomy Monthly Notices of the Royal Astronomical Society 197:507–511

Barlow F, Wood J, Elshabini A, Stephens E F, Feeler R, Kemner G & Junghans J (2009) Fabrication of Precise Fluidic Structures in LTCC International Journal of Applied Ceramic Technology 6 (1): 18–23.

Bryant A, Poirier M, Lee D, & Vetelino J (1982). A Surface Acoustic Wave Gas Detector. 36th Annual Symposium on Frequency Control 276-283.

Brüel & Kjær, Denmark http://www.bksv.com/Products/TransducersConditioning/vibration-transducers/accelerometers/accelerometers/4524.aspx?tab=specifications accessed 30.08.2012

Cady W (1964) Piezoelectricity. New York: Dover Publications.

Canon (2012) Technical Room - USM. http://www.canon.com/camera-museum/tech/room/usm.html. Cited 2013/04/03.

Chunsheng Z (2011) Ultrasonic motros. Technologies and Applications. Beijing: Springer.

Das R (2012) Piezoelectric energy harvesting market to reach $145 million in 2018. Energy Harvesting Journal. http://www.energyharvestingjournal.com/articles/piezoelectric-energy-harvesting-market-to-reach-145-million-in-2018-00004664.asp?sessionid=1. Cited 2013/04/03

Dogan A, Fernandez JF, Uchino K, & Newnham RE (1996) The "Cymbal" electromechanical actuator. Proceedings of the Tenth IEEE International Symposium on Applications of Ferroelectrics ISAF '96 213-216.

Dong S, Lim S, Lee K, Zhang J, Lim L, & Uchino K (2003) Piezoelectric Ultrasonic Micromotor with 1.5 mm Diameter. IEEE Transaction on Ultrasonics, Ferroelectrics, and Frequency Control 50(4): 361-367.

Endevco a, USA, http://elcodis.com/parts/5932901/2258AM2-10.html#datasheet accessed 30.08.2012

Endevco b, USA, https://www.endevco.com/product/prodpdf/7267A_.pdf accessed 30.08.2012

Endevco c, USA, https://www.endevco.com/product/prodpdf/7268C.pdf accessed 30.08.2012

Elfrink R, Kamel TM, Goedbloed M, Matova S, Hohlfeld D, Andel Y, & van Schaijk R (2009) Vibration energy harvesting with aluminum nitride-based piezoelectric devices. Journal of Micromechanics and Microengineering 19(9): 1-8.

Ferroperm Piezoceramics. Product catalog. http://app04.swwwing.net/files/files/Ferroperm%20Catalogue.pdf. Cited 2013/04/03.

Flossel M, Scheithauer U, Gebhardt S, Schonecker A, & Michaelis A (2009) Robust LTCC/PZT sensor-actuator-module for aluminium die casting. Microelectronics and Packaging Conference, 2009. EMPC 2009 1-5.

Fournier Y, Seigneur F, Maeder T, & Ryser P (2007) Assembly of microvalves actuated by PZT bender. Proceedings, International Conference on Electroceramics (ICE2007), Arusha, Tanzania.

Germano C (1971) Flexure mode piezoelectric transducers. IEEE Transactions on Audio and Electroacoustics 19(1): 6-12.

Golonka L, Roguszczak H, Zawada T, Radojewski J, Grabowska I, Chudy M & Stadnik D (2005) LTCC based microfluidic systems with optical detection. Sensors and Actuators B 111-112: 396-402.

Gongora-Rubio MR, Espinoza-Vallejos P, Sola-Laguna L & Santiago-Avilés JJ (2001) Overview of low temperature co-fired ceramics tape technology for meso-system technology (MsST). Sensors and Actuators A: Physical 89(3): 222-241.

Gongora-Rubio MR, Fontes MB, Rocha ZM, Richter EM & Angnes L (2004) LTCC manifold for heavy metal detection system in biomedical and environmental fluids. Sensors and Actuators B: Chemical 103(1-2): 468-473.

Hayamizu S, Higashino K, Fujii Y, & Yamamoto K (2003) Development of a bi-directional valve-less silicon micro pump controlled by driving waveform. Sensors and Actuators A: Physical 103(1-2): 83-87.

Heinonen E, Juuti J & Jantunen H (2007) Characteristics of piezoelectric cantilevers embedded in LTCC. Journal of the European Ceramic Society 27(13-15): 4135-4138.

Heraeus Advanced Materials HeraLock Tape HL2000 http://www.heraeus-thickfilm.com/media/webmedia_local/media/datasheets/ltccmaterials/HL2000.pdf Cited 2013/04/03.

Hindrichsen C, Larsen J, Thomsen E, Hansen K, Lou-Møller R (2009) Circular Piezoelectric Accelerometer for High Band Width Application, IEEE SENSORS 2009 Conference Proceedings 475-478

Hindrichsen C, Almind N, Brodersen S, Lou-Møller R, Hansen K, Thomsen E (2010) Triaxial MEMS accelerometer with screen printed PZT thick film. Journal of Electroceramics 25:108-115.

Hirooka D, Suzumori K & Kanda T (2009) Flow control valve for pneumatic actuators using particle excitation by PZT vibrator. Sensors and Actuators A: Physical 155(2): 285-289.

Howells C (2009) Piezoelectric energy harvesting. Energy Conversion and Management 50(7): 1847-1850.

Hrovat M, Holc J, Drnovšek S, Belavič D, Cilenšek J & Kosec M (2006) PZT thick films on LTCC substrates with an interposed alumina barrier layer. Journal of the European Ceramic Society 26(6): 897-900.

Imanaka Y (2005) Multilayerd Low Temperature Cofired Ceramics (LTCC) Technology. Springer.

Jaffe B, Cook W & Jaffe H (1971) Piezoelectric ceramics. New York: Academic Press.

Jurkow D, Dabrowski A, Golonka L, Zawada T (2013) Preliminary Model and Technology of Piezoelectric Low Temperature Co-fired Ceramic (LTCC) Uniaxial Accelerometer, International Journal of Applied Ceramic Technologies 10:395–404

Juuti J, Jantunen H, Moilanen VP & Leppavuori S (2006) Manufacturing of prestressed piezoelectric unimorphs using a postfired biasing layer. IEEE Transactions on Ultrasonics, Ferroelectrics and Frequency Control, 53(5): 838-846.

Juuti J, Jantunen H, Moilanen VP & Leppävuori S (2005) Poling conditions of prestressed piezoelectric actuators and their displacement. Journal of Electroceramics 15: 57-64.

Kara D. Optical fiber switch made in LTCC technology (2004) Wroclaw University of Technology, Thesis Work

King WH (1964) Piezoelectric Sorption Detector. Analitical Chemistry 36(9): 1735-1739.

Kistler, Switzerland, http://www.kistler.com/mediaaccess/8395A10__000-860a-07.11.pdf accessed 30.08.2012

Kok S, White NM & Harris NR (2009) Fabrication and characterization of free-standing thick-film piezoelectric cantilevers for energy harvesting. Measurement Science & Technology 20(12): 124010-124023.

Lautzenhiser F, Amaya E & Hochheimer T (2004) Self-constrained low temperature glass-ceramic unfired tape for microelectronics and methodes for making and using the same. US Patent nrUS 2003/0087136 A1.

Li S, Shaanxi X & Lipson H (2009) Verrtical-stalk flapping-leaf generator for wind energy harvesting. Proceedings of the ASME 2009 Conference on Smart Materials, Adaptive Structures and Intelligent Systems 1-9.

Lim C, Wang W, Yang S & Lee K (2011) Development of SAW-based multi-gas sensor for simultaneous detection of CO2 and NO2. Sensors and Actuators B: Chemical 154(1): 9-16.

Malecha K, Pijanowska DG, Golonka LJ & Torbicz W (2009) LTCC microreactor for urea determination in biological fluids. Sensors and Actuators B: Chemical 141(1): 301-308 .

Matatagui D, Martí J, Fernández MJ, Fontecha JL, Gutiérrez J, Gràcia I & Horrillo MC (2011) Chemical warfare agents simulants detection with an optimized SAW sensor array. Sensors and Actuators B: Chemical 154(2): 199-205.

Metra Mess- und Frequenzrechnik in Radebeul e.K., Triaxial Accelerometers. URL: http://www.mmf.de/triaxial_accelerometers.htm accessed 30.08.2012

Mistler RE & Twiname ER (2000) Tape Casting, Theory and Practice. Westerville: The American Ceramic Society.

Mulder BJ (1984) Simple piezoelectric microbalance based on a vibrating quartz wire. Journal of Physics E: Scientific Instruments, 17(2).

Niezrecki C, Brei D, Balakrishnan S & Moskalik A (2001) Piezoelectric Actuation: State of the Art. The Shock and Vibration Digest 33(4): 269-280.

Patterson J (1997) Micro-mechanical voltage tunable Fabry–Perot filters formed in (111) silicon Nasa Langley Research Center, Hampton, WV, Nasa technical paper 3702

Peng TJ, Yang GZ, Cheng GM, Kan JW & Zeng P (2009) Design of double-chamber piezoelectric pump. Optics and Precision Engineering, 17(5), 1078-11085.

Prusak-Sochaczewski E, Luong JH & Guilbault GG (1990) Development of a piezoelectric immunosensor for the detection of Salmonella typhimurium. Enzyme and Microbial Technology 12(3): 173-177.

Rabe T, Schiller W, Hochheimer T, Modes C & Kipka A (2005) Zero Shrinkage of LTCC by Self-Constrained Sintering. International Journal of Applied Ceramic Technology 2(5): 374-382.

Reay R, Ring J, Seaddan R (1974) A Tunable Fabry–Perot filter for the visible J. Phys. E Sci. Instrum 7(8): 673–677

Santo Zarnik M & Belavic D (2005) Design Study for a Thick-Film Piezoelectric Actuator in an LTCC Structure. Proceedings in 6th. Int. Conf. on Thermal, Mechanical and Mubiphysics Simulation ond Experiments in Micro-Elecfmnics ond Micro-System, EumSimE 2005, 338-346.

Sari I, Balkan T & Kulah H (2008) An electromagnetic micro power generator for wideband environmental vibrations. Sensors and Actuators A: Physical 145-146: 405-413.

Seiko Instruments Inc. (2013) Ultrasonic Micromotor -- Seiko Instruments Inc. http://www.sii.co.jp/info/eg/micro-usm1.html. Cited 2013/04/03.

Silicon designs, USA, http://www.directindustry.com/prod/silicon-designs/triaxial-capacitive-accelerometers-20945-462051.html accessed 30.08.2012

Spetz A (2006) Chemical Sensor Technologies, Tutorial 2006. http://hermes.material.uu.se/~klas/Chemical%20Sensor%20Technologies%202006.pdf . Cited 2013/04/03.

Sugawara Y, Onitsuka K, Yoshikawa S, Xu Q, Newnham RE & Uchino K (1992) Metal–Ceramic Composite Actuators. Journal of the American Ceramic Society 75(4): 996-998.

Takahashi S, Ochi A, Yonezawa M, Yano T, Hamatsuki T & Fukui I (1983) Internal electrode piezoelectric ceramic actuator. Ferroelectrics 50(1): 181-190.

Tick T, Palukuru V, Komulainen M, Peräntie J & Jantunen H (2008). Method for manufacturing embedded variable capacitors in low-temperature cofired ceramic substrate. Electronics Letters 44(2): 94-95.

Uchino K (2000) Ferroelectric devices. New York: Marcel Dekker.

Wagner J & Burgemeister J (2012). Piezoelectric Accelerometers. Theory and Application. 6th edition. Metra Mess- und Frequenztechnik. Radebeul: Manfred Weber Metra Mess- und Frequenztechnik.

Wang HW, Cheng SY & Wang CM (1989) Optimization of poling process for piezoelectric PZT ceramics. Proceedings of Sixth IEEE/CHMT International Electronic Manufacturing Technology Symposium 1989, 263-266.

Wohltjen H & Dessy R (1979) Surface acoustic wave probe for chemical analysis. Analytical Chemistry 51(9): 1458-1464.

Wu TZ (1999) A piezoelectric biosensor as an olfactory receptor for odour detection: electronic nose. Biosensors and Bioelectronics 14(1): 9-18.

Yang X, Zhou Z, Cho H & Luo X (2005) Study on a PZT-actuated diaphragm pump for air supply for micro fuel cells. Sensors and Actuators A: Physical 130-131: 531-536.

Yu B, Pickrell G, Woong Kim D, Wang A (2004) Thermally tunable extrinsic Fabry–Perot filter for white-light interferometry Frontiers in Optics

Yun S, Lee K, Kim H & So H (2006) Development of the pneumatic valve with bimorph type PZT actuator. Materials Chemistry and Physics 97(1): 1-4.

Zampetti, E, Pantalei S, Macagnano A, Proietti E, Di Natale C & D'Amico A (2008) Use of a multiplexed oscillator in a miniaturized electronic nose based on a multichannel quartz crystal microbalance. Sensors and Actuators B: Chemical 131(1): 159-166.

Original Papers

I Sobociński Maciej, Zwierz Radoslaw, Juuti Jari, Jantunen Heli, Golonka Leszek (2010) Electrical and electromechanical characteristics of LTCC embedded piezoelectric bulk actuators. Advances in Applied Ceramics Volume 109, Pages 135 – 138.

II Sobocinski Maciej, Leinonen Mikko, Juuti Jari and Jantunen Heli (2011) Monomorph piezoelectric wideband energy harvester integrated into LTCC. Journal of the European Ceramic Society, Volume 31, Issue 5, Pages 789 - 794

III Sobocinski Maciej, Leinonen Mikko, Juuti Jari, Jantunen Heli (2012) A Piezoelectric active mirror suspension embedded into Low Temperature Co-fired Ceramic. IEEE Transactions on Ultrasonics, Ferroelectrics, and Frequency Control, Volume 59, Number 9, Pages. 1990 – 1995

IV Sobocinski Maciej, Leinonen Mikko, Juuti Jari, Mantyniemi Noora, Jantunen Heli (2014) A Co-fired LTCC-PZT monomorph bridge type acceleration sensor. Sensors and Actuators A, Physical, 216

V Sobociński Maciej, Juuti Jari, Jantunen Heli, Golonka Leszek (2009) Piezoelectric unimorph valve assembled on an LTCC substrate. Sensors and Actuators. A, Physical. 2009, Volume 149, Number 2, Pages 315-319

Original papers are not included in the electronic version of the dissertation.

497. Myllylä, Teemu (2014) Multimodal biomedical measurement methods to study brain functions simultaneously with functional magnetic resonance imaging
498. Tamminen, Satu (2014) Modelling the rejection probability of a quality test consisting of multiple measurements
499. Tuovinen, Lauri (2014) From machine learning to learning with machines : remodeling the knowledge discovery process
500. Hosio, Simo (2014) Leveraging Social Networking Services on Multipurpose Public Displays
501. Ohenoja, Katja (2014) Particle size distribution and suspension stability in aqueous submicron grinding of $CaCO_3$ and TiO_2
502. Puustinen, Jarkko (2014) Phase structure and surface morphology effects on the optical properties of nanocrystalline PZT thin films
503. Tuhkala, Marko (2014) Dielectric characterization of powdery substances using an indirectly coupled open-ended coaxial cavity resonator
504. Rezazadegan Tavakoli, Hamed (2014) Visual saliency and eye movement : modeling and applications
505. Tuovinen, Tommi (2014) Operation of IR-UWB WBAN antennas close to human tissues
506. Vasikainen, Soili (2014) Performance management of the university education process
507. Jurmu, Marko (2014) Towards engaging multipurpose public displays : design space and case studies
508. Namal, Suneth (2014) Enhanced communication security and mobility management in small-cell networks
509. Huang, Xiaohua (2014) Methods for facial expression recognition with applications in challenging situations
510. Ala-aho, Pertti (2014) Groundwater-surface water interactions in esker aquifers : from field measurements to fully integrated numerical modelling
511. Torabi Haghighi, Ali (2014) Analysis of lake and river flow regime alteration to assess impacts of hydraulic structures
512. Bordallo López, Miguel (2014) Designing for energy-efficient vision-based interactivity on mobile devices

Book orders:
Granum: Virtual book store
http://granum.uta.fi/granum/

UNIVERSITY OF OULU P.O. Box 8000 FI-90014 UNIVERSITY OF OULU FINLAND

A C T A U N I V E R S I T A T I S O U L U E N S I S

ISBN 978-952-62-0703-2 (Paperback)
ISBN 978-952-62-0704-9 (PDF)
ISSN 0355-3213 (Print)
ISSN 1796-2226 (Online)

UNIVERSITY of OULU
OULUN YLIOPISTO